On the relation of phase separation and Hi-C maps to epigenetics

By

Prim B. Singh[1*,2,3] and Andrew G. Newman[3]

[*1]Nazarbayev University School of Medicine,
5/1 Kerei, Zhanibek Khandar Street,
Nur-Sultan Z05K4F4,
Kazakhstan

[2]Epigenetics laboratory,
Department of Natural Sciences,
Novosibirsk State University,
Pirogov str. 2,
Novosibirsk 630090,
Russian Federation

[3]Institute of Cell and Neurobiology,
Charité – Universitätsmedizin Berlin,
Corporate member of Freie Universität Berlin,
Humboldt-Universität zu Berlin and Berlin Institute of Health,
Berlin,
Germany

[*]Corresponding author: prim.singh@nu.edu.kz

Abstract

The relationship between compartmentalisation of the genome and epigenetics is long and hoary. In 1928 Heitz defined heterochromatin as the largest differentiated chromatin compartment in eukaryotic nuclei. Müller's (1930) discovery of position-effect variegation (PEV) went on to show that heterochromatin is a cytologically-visible state of heritable (epigenetic) gene repression. Current insights into compartmentalisation have come from a high-throughput top-down approach where contact frequency (Hi-C) maps revealed the presence of compartmental domains that segregate the genome into heterochromatin and euchromatin. It has been argued that the compartmentalisation seen in Hi-C maps is due to the physiochemical process of phase separation. Oddly, the insights provided by these experimental and conceptual advances have remained largely silent on how Hi-C maps and phase separation relate to epigenetics. Addressing this issue directly in mammals, we have made use of a bottom-up approach starting with the hallmarks of constitutive heterochromatin, heterochromatin protein 1 (HP1) and its binding partner the H3K9me2/3 determinant of the histone code. They are key epigenetic regulators in eukaryotes. Both hallmarks are also found outside mammalian constitutive heterochromatin as constituents of larger (0.1-5Mb) heterochromatin-*like* domains and smaller (less than 100Kb) complexes. The well-documented ability of HP1 proteins to function as bridges between H3K9me2/3-marked nucleosomes enables cross-linking within and between chromatin fibres that contributes to polymer-polymer phase separation (PPPS) that packages epigenetically-heritable chromatin states during interphase. Contacts mediated by HP1 "bridging" are likely to have been detected in Hi-C maps, as evidenced by the B4 heterochromatic sub-compartment that emerges from contacts between large KRAB-ZNF heterochromatin-*like* domains. Further, mutational analyses have revealed a finer, innate, compartmentalisation in Hi-C experiments that likely reflect contacts involving smaller domains/complexes. Proteins that bridge (modified) DNA and histones in nucleosomal fibres – where the HP1-H3K9me2/3 interaction represents the most evolutionarily-conserved paradigm – could drive and generate the fundamental compartmentalisation of the interphase nucleus. This has implications for the mechanism(s) that maintains cellular identity, be it a terminally-differentiated fibroblast or a pluripotent embryonic stem cell.

Keywords: Heterochromatin, polymer-polymer phase separation, contact frequency maps, Hi-C maps, epigenetics, block copolymers, HP1, H3K9me2/3, nucleosome, chromatin fibres.

Background

Cursory inspection of eukaryotic nuclei using a simple light microscope shows that the optical density of chromatin is not uniform. On this basis Emil Heitz (1) defined heterochromatin as the dense compartment that is opaque to transmitted light and stains deeply with simple dyes, while euchromatin was the other compartment that stained lightly and through which light passed readily. Beyond this strictly empirical definition, quantitative techniques have shown that DNA in mammalian interphase nuclei is indeed more densely packed in constitutive heterochromatin compared with euchromatin. There is two- to six-fold higher density of DNA in heterochromatin as measured by fluorescence intensity of DNA-binding fluorophores (2, 3), which can be confirmed by measuring nucleosome density using fluorescently-tagged histones (3, 4). The increased nucleosome density reflects how the 11-nm "beads-on-a-string" nucleosome fibre is packaged in heterochromatin. And recent work provides a pathway that might explain the increased density observed. In H3K9me3-marked heterochromatin the preferred contact geometry of the nucleosome fibre is a two start helical fibre with stacked alternating nucleosomes, making the closest neighbour the second nearest nucleosome rather than next nearest nucleosome (5). Super-resolution imaging has revealed another level of organisation that is characterised by the assembly of irregularly folded "clutches" of nucleosomes where the density of larger "clutches" is greater in heterochromatin compared to euchromatin (6). The molecular crowding observed in the heterochromatic environment (2, 4) has been modelled and predicted to enhance the interaction between the "clutches" due to osmotic depletion attraction (7). The calculated entropy-driven attraction is small, ~$0.5k_BT$, but could favour the merging of "clutches" to form ordered (fractal) "globules" that have been detected by chromosome conformation capture (8, 9) and super-resolution imaging (10).

Soon after Heitz's definition of heterochromatin Hermann Müller (11) discovered the phenomenon of ever-sporting displacements in *Drosophila*, later called position-effect variegation (PEV). PEV continues to be an important experimental paradigm for interrogating the relationship of constitutive heterochromatin to euchromatin in a living animal by disrupting the natural boundary that separates the two cytologically-distinguishable states of chromatin (reviewed in (12–15)). PEV led to key conceptual advances and generated invaluable molecular tools that have done much to provide an outline of the natural history of constitutive heterochromatin by unveiling conserved mechanisms that operate in species ranging from fission yeast to man (16, 17). Outstanding amongst the contributions of PEV were, first, the demonstration that the effect of constitutive heterochromatin on gene repression is pervasive and heritable. Pervasive because, in most cases of PEV, repression results from "spreading" of the dense packaging from within constitutive heterochromatin across the variegating breakpoint into euchromatin (18–20). Once established, repression is heritable from one cellular generation to the next (21, 22). Thus the discovery of PEV (11) gave birth to the discipline of *epigenetics* more than a decade before the term itself was coined (23). Second, was the identification of second-

site modifiers of variegation that encode structural and enzymatic components of constitutive heterochromatin (reviewed in (15, 24)). Two of these modifiers encode proteins that are highly-conserved in organisms from fission yeast to man. One is heterochromatin protein 1 (HP1) and the other H3K9 HMTases that generate the H3K9me2/3 determinant of the histone code to which HP1 binds (25). HP1 and H3K9me2/3 are hallmarks of constitutive heterochromatin and key epigenetic regulators in eukaryotes (16, 17). They represent a potential link between compartmentalisation and epigenetics that will be explored in this paper. We now turn to these hallmarks with a focus on mammalian HP1 proteins because recent *in vitro* work has indicated that they form liquid-liquid condensates and gel-like states (26–28) that could drive compartmentalisation of cytologically-visible constitutive heterochromatin in interphase nuclei.

Mammalian HP1 proteins and polymer-polymer phase separation (PPPS)

In mammals there are three HP1 isotypes, termed HP1α, HP1β and HP1γ, which are encoded by distinct genes, chromobox homolog 5 (*Cbx5*), *Cbx1*, and *Cbx3*, respectively (29). Immuno-localisation studies have shown that HP1α and HP1β are usually enriched within constitutive heterochromatin (30), where their concentration is around 10μM (3). HP1γ has a more euchromatic distribution (30). They are small ~25kD molecules that consist of two globular domains, an N-terminal chromo domain (CD) and a sequence-related C-terminal chromo shadow domain (CSD), linked by an unstructured, flexible, hinge region (HR) (31). Depending on the species and isoforms there are less well-conserved N- and C-terminal extensions (NTE and CTE respectively) (Figure 1A). The CD specifically binds to the N-terminal tail of histone H3, when methylated at the lysine 9 residue (H3K9me) (32–34), with the highest (μM) affinity for the *tri*-methylated form (H3K9me3; (35); Figures 1B and C). From the crystallographic data the methyl-ammonium group in K9H3 is caged by three aromatic side chains in the CD, where the binding energy is driven largely by cation-π interactions (36) (Figure 1D). The CSD dimerizes and forms a ‘‘nonpolar’’ pit that can accommodate penta-peptides with the consensus sequence motif PxVxL, found in many HP1-interacting proteins (37–39) (Figures 1E to G). There are likely to be other modes of interaction with the nucleosome including, for example, that of the HP1 CD or CSD with the H3 histone “core” (40–42), binding of the HR region to DNA and RNA (43–45) and a non-specific electrostatic interaction of the NTE with the H3 tail (46).

Mutational analysis in mice has shown that mammalian HP1 isotypes have different mutant phenotypes despite sharing extensive sequence identity (29, 47). HP1α function is essentially redundant. *Cbx5*$^{-/-}$ mice are viable and fertile (cited in (48)) (47) albeit they exhibit a very specific defect where T_H1 expression is not silenced in T_H2 cells (49). HP1β function cannot be compensated by HP1α and γ. The *Cbx1*$^{-/-}$ mutation is fully penetrant with mice dying around birth possessing a variety of lesions including a severe genomic instability

(47). Disruption of the *Cbx3* gene (encoding HP1γ) results in infertility and an increased postnatal mortality (50–52). Consistent with the mutational analysis, unbiased exome data predicts HP1β to have the highest probability of loss of function intolerance (pLI) out of the HP1 proteins* (53).

Mammalian HP1 proteins were some of the first proteins used in non-invasive FRAP studies to probe chromatin protein interactions in living cells (54). Numerous FRAP studies, in conjunction with kinetic modelling, have shown that at steady state equilibrium the nuclear HP1 pool can be separated into three kinetic fractions: a highly mobile ''fast'' fraction that freely diffuses through the nucleoplasm, a less mobile ''slow'' fraction that binds to the HP1 ligand, H3K9me3 in heterochromatin, and a small immobile HP1 fraction whose ligand(s) is not known (55–57), although it has been suggested that this tightly bound fraction may involve the interaction of HP1 proteins with the histone H3 "core" (58, 59). These data have been interpreted as heterochromatin being a stable, membrane-less, nuclear compartment whose structural integrity is mediated by protein-protein and protein-RNA interactions, where the bulk of the constituents exchange freely with the surrounding nucleoplasm (60). This view presages thermodynamic models of intracellular phase separation, which have led to physiochemical explanations for the biogenesis and maintenance of different nuclear compartments found in living cells (reviewed in (61–64)).

An exemplar of a nuclear compartment that is formed by liquid-liquid phase separation (LLPS) is the nucleolus, which is assembled at transcriptionally active ribosomal DNA loci (65, 66). Detailed examination of nucleoli has shown they are not composed of a single condensed phase surrounded by a dilute phase but consist of sub-compartments where a secondary condensed phase is contained within the primary condensed phase; the sub-compartments have distinct viscosities, surface tensions and protein compositions (67, 68). *in vitro* studies on mammalian HP1α have shown that HP1α undergoes LLPS and led to the suggestion that HP1α-dependent constitutive heterochromatin might also consist of phase separated sub-compartments, specifically a soluble phase, a liquid droplet phase and a gel-like phase (27, 28). The propensity to form liquid droplets *in vitro* is peculiar to HP1α because, under the same conditions, HP1β and γ do not form liquid droplets (69); there seems not to be a relationship between the ability to form liquid droplets and pLI. On the face of it, the three phase-separated HP1α sub-compartments appear to correspond with the three kinetic fractions observed in FRAP studies. However, a notable difference is that mammalian HP1α liquid droplets form *in vitro* independently of chromatin (26, 28) while the "slow" fraction is dependent upon the *in vivo* interaction of HP1 with its ligand, H3K9me3 (55, 57). Crucially, the CasDrop system has shown that mammalian HP1α is unlikely to form liquid

* pLI is a probability calculation of how well loss of function mutations can be tolerated, where 1.00 means the loss of function of the protein cannot be tolerated. HP1β holds a pLI of 0.95 while HP1α a lower pLI of 0.84, and HP1γ a pLI of 0.63

droplets *in vivo* (70). Instead, HP1α-rich foci co-localise with constitutive heterochromatin (30) rather than forming droplets that surround heterochromatin (70) indicating that if HP1α does drive phase separation it does so in a manner different from multivalent intrinsically-disordered proteins (63), which are known to form endogenous liquid-liquid phase separated condensates in the nucleus (70). Based on these data we propose an alternative mechanism. Mammalian HP1 proteins drive phase separation by polymer-polymer phase separation (PPPS; (71)) rather than by LLPS.

Evidence that LLPS is unlikely to be the mechanism by which HP1 proteins form phase separated compartments also comes from studies on their ability to act as bridging molecules between distant chromosomal loci. Expression of a lacI-HP1βCD fusion in a mouse cell line harbouring a ~10kB lac operator (*lacO*; (72)) integrated into the telomeric end of chromosome 11 increased the frequency of contacts between the lacI-HP1βCD fusion bound to the *lacO* allele and H3K9me3-marked peri-centromeric heterochromatin (73). The bridging effect requires the CD-H3K9me3 interaction because a point mutation (T51A in HP1βCD) that disrupts the interaction of the CD with H3K9me3 decreased the frequency of contacts to that observed for the wild-type (wt) allele. This ability of HP1 proteins to promote contact between distant chromosomal loci is conserved. Using the same *lacO* system a transgenic fly was generated where *lacO* was integrated into the telomeric end of the X-chromosome (74). Expression of a lacI-HP1a fusion led to a discrete lacI-HP1a signal at *lacO* on polytene chromosomes (74). Assembly of lacI-HP1a at the *lacO* promoted chromosome folding and association of the lacI-HP1a-*lacO* complex with loci at distant chromosomal sites. Bridging between two loci was dependent upon HP1a CSD dimerization. The bridging effect in transgenic flies was all the more impressive given it was observed in polytene chromosomes, which do not fold easily because of their stiffness that is a consequence of the ~1000 sister chromonemata that align in complete register, resulting in the giant cross-banded chromosomes (75); a lack of flexibility (increased stiffness) is the reason given for the absence of compartmental domains in Hi-C maps generated from polytene nuclei (76). It is unlikely that HP1a liquid droplets could mediate this long-range bridging effect. For one, a liquid droplet would surround chromatin whereas the lacI-HP1a forms a tightly-localised domain at *lacO* (74). Further, the bridging effects observed *in vitro* and *in vivo* are mediated by direct stereospecific interactions requiring the modular domains of HP1 (73, 74, 77), whereas liquid droplets pull genomic regions together by proxy *via* surface tension driven coalescence (70).

The 11-nm nucleosome fibre is a polymer (78, 79). The physics of polymers is well understood and predicts that very small interactions between monomers can strongly influence the whole structure because many small interactions can add up to stabilize different structures (80, 81). For example, when a homo-polymer is

placed in a solvent the interaction of monomers with themselves and the solvent can lead to an incompatibility that results in phase separation of the polymer (*i.e.*, the polymer de-mixes because the energetic cost of mixing the polymer in the solvent is prohibitive), whereupon the polymer collapses into structures such as ordered globules surrounded by a solvent-rich phase (80–84). Notably, the formation of ordered globules is likely to be one of the consequences of folding of the nucleosome fibre "polymer" in the nucleus. This was concluded from the first Hi-C study, which showed that the average contact probability $P_c(s)$ between two loci at a distance *s* is a power law, $P_c(s) \sim 1/s^{\alpha}$, having a specific exponent $\alpha = 1.08$ for genomic distances up to the size of several Mb (8). This observation led to the notion that the nucleosome fibre adopts a specific state found in ideal polymer chains models, namely the ordered (fractal) globule, which has an exponent $\alpha = 1$ (84). Scaling of s^{-1} is best understood in terms of the nucleosome fibre folding into small 'globular' regions which condense into larger globules that then form even larger globules (84) (Figure 6). The resulting structure is self-similar (*i.e.*, fractal) over two orders of magnitude from around the level of whole chromosomes down to a scale of a few hundred Kb (8). Subsequent Hi-C studies have shown that the exponent can vary depending on cell type indicating that the nucleus contains a complex mixture of differently folded regions, including ordered (fractal) globules, controlled by basic mechanisms of polymer physics that are strongly influenced by chromatin binding proteins and epigenetic modifications (85).

When homo-polymers in solution are cross-linked they can form condensed structures that are incompatible with the surrounding solvent, resulting in de-mixing and phase separation (86, 87). Highly cross-linked chromatin, such as that found in mitotic chromosomes, forms phase separated polymer gels (88). Similarly, phase separation could arise when H3K9me2/3-marked nucleosome "polymers" are cross-linked by HP1-mediated "bridging" within and between the "polymer" fibres. Bridging by HP1 proteins has been definitively demonstrated through elucidation of the three-dimensional structure of H3K9me3-containing di-nucleosomes complexed with human HP1α, β or γ (77) (Figure 2). Two H3K9me3 nucleosomes are bridged by a symmetric HP1 dimer *via* the H3K9me3-CD interaction; the linker DNA between the nucleosomes does not directly interact with HP1 (77). *in vivo* FRAP studies indicate that the binding of HP1 to H3K9me3-marked nucleosomes is dynamic and transient but the rapid and constant exchange with unbound HP1 in the nucleoplasm (55–57) would maintain the bridging interactions. Given the rapid turnover of H3K9me3-bound HP1, HP1-mediated bridging may stabilise or promote pre-existing (condensed) chromatin compaction states rather than inducing these states *de novo*. Notably, the interaction of HP1α and β with H3K9me3-marked nucleosomal fibres revealed that HP1 dimers can bridge different segments of the same fibre (46, 74). HP1 dimers can also bridge between H3K9me3-marked nucleosomal fibres *i.e.*, drive inter-fibre interactions (46, 74). Given the flexible HR, HP1-bridging could promote or stabilize the conformation of H3K9me3 marked

nucleosome fibers, within and between larger "clutches" of nucleosomes that are known to be enriched in heterochromatin (5, 6) (Figure 3). Together with osmotic depletion attraction (7) the HP1-mediated bridging (cross-linking) between "clutches" would promote their coalescence with the potential to form/stabilize (fractal) globules (Figure 3) that could contribute to PPPS of constitutive heterochromatin.

Constitutive heterochromatin, heterochromatin-*like* domains and complexes

Constitutive heterochromatin is found at distinct chromosomal territories - around the centromeres (peri-centromeric), at the telomeres and flanking the peri-nucleolar regions (for reviews see (89–92)). They are huge, ranging up to 20Mb in size in mouse and man (Table 1). Their size makes them cytologically-visible, which enabled Heitz (1) to demonstrate graphically compartmentalisation of the eukaryotic genome. In mammals, the bulk surrounds the centromeres (peri-centromeric) and, surprisingly, there is no conserved sequence one can point to that is known to cause nucleation at this site. Instead, it is thought the generally-repetitious nature of sequences promotes nucleation of peri-centromeric constitutive heterochromatin (89). In addition to repetitious DNA there are proteins, RNAs and epigenetic modifications enriched within constitutive heterochromatin (93, 94) (Table 1) that are thought to be involved its nucleation, assembly and propagation (89). Several of these constituents may contribute to PPPS of constitutive heterochromatin the most likely, but not exclusively, being affinity of homotypic DNA repetitive elements for each other (95), mutual affinity of nucleosomes that share the same modified histones and proteins that bridge between DNA and nucleosome fibres. Along with HP1 proteins, bridging is a property shared by many other proteins that possess two (or more) chromatin/DNA binding motifs (96, 97), any of which could contribute to PPPS of constitutive heterochromatin. For example, methyl binding proteins might contribute by bridging methylated nucleosomal DNA fibres (3). Putting it short, there are several factors that are likely to contribute to PPPS of cytologically-visible constitutive heterochromatin, with the hallmarks HP1 and H3K9me2/3 being the most conserved.

The demonstration that genes encoding HP1 proteins are highly-conserved was accompanied by the prediction that HP1-containing heterochromatin-*like domains* and *complexes* would exist *outside* canonical constitutively heterochromatic territories and regulate the cell-to-cell (epigenetic) inheritance of chromatin states (98) (for reviews see (29, 59, 99, 100)). Many such domains and complexes that share structural components (*e.g.* HP1) and epigenetic modifications (*e.g.* H3K9me3) have been identified now (Table 1). An attempt at a rough classification as a domain or complex has been made on the basis of size (100), with *domains* being in the region of ~ 0.1-5Mb in size (Table 1). Included in the *domains* are the odorant receptors (101–103), the KRAB-ZNF gene clusters (104) contained within the B4 sub-compartment (105); the protocadherin topologically associated domain (TAD; (106)), somatic cell nuclear transfer (SCNT) Reprogramming Resistant Regions (RRRs; (107)) and the Zscan4 gene cluster (108). There is evidence that these domains assemble regions of

chromosomal DNA involved in regulating cell fate (109, 110). Moreover, perturbation in their assembly and propagation is likely to affect cellular identity (111, 112) and SCNT reprogramming efficiency (107). Heterochromatin-*like complexes* are small, less that 100kB and usually only a few kB in size (Table 1). They include the 3' end of the KRAB-ZNF genes (104, 113), imprinted gDMRs (114) and the SETDB1-regulated iPS reprogramming resistant regions (115). The targeted assembly of these domains/complexes contributes to the coarse-grained chromatin-state pattern that characterizes mammalian genomes (116, 117).

There are four different but related questions that need to be addressed in order to understand how heterochromatin-*like* domains/complexes regulate chromatin-templated processes and genome organisation. First, how is the assembly of a heterochromatin-*like* domain/complex nucleated at a particular site in the genome? Second, how does a larger domain form by spreading along the nucleosome fibre from that site? Third, how is the domain/complex epigenetically inherited from one cellular generation to the next? And finally, how do such domains/complexes contribute to compartmentalisation of the genome in terms of heterochromatin and euchromatin? Clues to what the answers might look like have come from studies on the heterochromatin-*like* domains that encompass the **Kr**üppel-**a**ssociated **b**ox (KRAB) domain zinc-finger (KRAB-ZNF) gene clusters (Table 1) (104). In humans, the majority of clusters reside on chromosome 19. The KRAB-ZNF genes encode the largest family of transcriptional regulators in higher vertebrates (118) and the general features of the heterochromatin-*like* domains that encompass the KRAB-ZNF genes clusters are well described. The mammalian HP1 protein, HP1β, and the K9 HMTase SUV39H1 are enriched at the KRAB-ZNF gene clusters and the 20 domains on human chromosome 19 range from 0.1 to 4Mb in size (104). HP1β binding is elevated throughout the clusters compared to regions outside the clusters and high-resolution analysis of a specific cluster on chromosome 19, encompassing the ZNF77 and ZNF57 genes, has shown that HP1β binding is co-extensive with H3K9me3 (113). Formation of large heterochromatin-*like* domains that encompass the clusters is thought to "protect" the KRAB-ZNF gene repeats as they have expanded during evolution by preventing illegitimate recombination (104), rather than to repress and silence the KRAB-ZNF genes (113, 119). Notably, there are significant variations along a cluster, with enrichment of HP1β at 3' end of KRAB-ZNF genes and depletion in the 5' promoter regions (104, 119). The enrichment observed at the 3' end has focussed attention on the molecular mechanism by which a heterochromatin-*like* domain can be nucleated, which brings us to the first of the four questions that need to be addressed.

A localised heterochromatin-like complex nucleates formation of the larger domain

Nucleation of the domain likely involves the assembly of a specific, localized, heterochromatin-*like* complex at the 3' end of the KRAB-ZNF genes (Table 1: Figure 4A). Nucleation is necessarily sequence-specific and intriguingly enough requires binding of a sequence-specific KRAB-ZNP to the 3' end of the

KRAB-ZNF genes (120, 121). Once bound to its cognate recognition sequence the KRAB-ZNP recruits the universal co-repressor of KRAB-ZNPs, KRAB-associated protein 1 (KAP1; also known as Tif1β, TRIM28 or KRIP1) (122–124); the KRAB motif of the DNA-bound KRAB-ZNP binds to the RBCC domain of KAP1 (122). KAP1 acts as a "scaffold" for different enzymatic and structural components that are essential for the nucleation process (Figure 4A). A key interaction is that of the SETDB1 HMTase with KAP1 that leads to the generation of the H3K9me3 modification (119, 121). SETDB1 binds the sumoylated form of the KAP1 bromodomain; the sumoylated version is the active, most repressive, form of KAP1 (125). Sumoylation is mediated intra-molecularly - the KAP1 PHD domain is an E3 ligase that co-operates with UBE2i (also known as UBC9) to transfer SUMO2 (126) to the KAP1 bromodomain. KAP1 also recruits a dimer of HP1 molecules through the PxVxL motif in KAP-1 called the HP1-box (127, 128); KAP1 binds equally well to all three HP1α/β/γ isotypes in biochemical assays (127, 128). Nucleation is reinforced by a specific mechanism that continually replenishes the repressive H3K9me3 modification. Specifically, KAP1 binds to DAXX (129), which is a H3.3 specific chaperone (130–132) that incorporates H3.3 at the 3' end of the KRAB-ZNF genes (133), whereupon H3.3 is tri-methylated at K9 by SETDB1 (121). Binding of the ATRX-DAAX complex is enhanced by the known interaction of ATRX with both H3K9me3 and HP1, the former through the ADD domain and the latter through an LxVxL motif, and both interfaces combine to localise ATRX to heterochromatin (134). The SETDB1-HP1-ATRX complex is stable *in vivo*: when HP1 is artificially repositioned within the nucleus both SETDB1 and ATRX are relocated along with it (135).

Several additional enzymatic activities likely to be part of the nucleation process have been revealed using artificially reconstituted systems where a regulatable KRAB domain is targeted to a synthetic sequence that drives a reporter gene (136–139). The small (~1.5kB) heterochromatin-*like* complexes generated by the targeted KRAB domains possess elevated levels of both H4K20me3 as well as H3K9me3 (138, 139) indicating the recruitment of a H4K20me3 HMTase and operation of the H3K9me3:HP1:H4K20me3 pathway (140). The KAP1 recruited by the KRAB domain also binds the NuRD complex that de-acetylates histones (136). There are also increased levels of DNA methylation (138, 141, 142), which is consistent with biochemical assays showing that KAP1 binds to all three DNA methyltransferases and the DNMT1 co-factor Np95 (143, 144); HP1 also interacts with all three DNA methyltransferases (145, 146).

Spreading to form a heterochromatin-like domain

Once a heterochromatin-*like* complex is nucleated at the 3'end of the KRAB-ZNF genes a larger domain is generated by "spreading" from that site through the activity of the SUV39H1 HMTase (104). Spreading moves away from the nucleation site towards the 5' end of the genes (113). SUV39H1 is the archetypal H3K9HMTase that generates the H3K9me3 to which HP1 binds (25). The most recent model posited for

SUV39H1-mediated spreading involves a "two-step" activation of SUV39H1 (147). First, a highly-mobile SUV39H1 with low HMTase activity attaches via its CD to H3K9me2/3 (Figure 4B, second panel) that would, in our scheme, be generated by the nucleation complex (Figure 4B, first panel). The second step involves H3K9 methylation of adjacent nucleosomes due to enhanced HMTase activity of the "anchored" SUV39H1 (Figure 4B, second panel). This mechanism is self-reinforcing because the SUV39H1CD binds newly-methylated H3K9 and in this way re-iterates along the nucleosome fibre, whereupon HP1 binds in its wake to the H3K9me3-marked nucleosomes (Figure 4B, third panel). The model is a refinement of earlier models where spreading involves a known interaction of SUV39H1 with HP1 (148, 149), where it is the CD of HP1 that binds newly methylated H3K9-nucleosomes and recruits SUV39H1 to re-inforce and continue spreading (32). HMTase-generated H3K9me3 "spreads" at the rate of ~0.18 nucleosomes/hr (150). The precise character of SUV39H1-mediated "spreading" has not been determined but it may be linear or involve a looping-driven propagation (147). We have depicted "spreading" as a looping-driven propagation (Figure 4B, third panel) in order to accommodate the "skipping" of the 5' end of the KRAB-ZNF genes where HP1β is depleted (104). Neither is it known how the spreading and thus domain size of the KRAB-ZNF clusters is limited, although several (boundary) sequence elements and associated proteins have been documented that can modulate the size and shape of heterochromatin domains (151, 152).

Genomic bookmarking and epigenetic inheritance

During mitosis HP1 proteins are removed from chromatin, only to re-associate in the following interphase (153). Consequently, in order for a heterochromatin-*like* domain to be epigenetically inherited from one cell generation to the next, the site at which it is nucleated in the genome must be "bookmarked" so that it is re-nucleated at that specific site after mitosis. Nucleation complexes (Figure 4A) are excellent candidates for genomic "bookmarks". They are assembled at specific sites through the binding of KRAB-ZNPs to their cognate recognition sequences (Figure 4A). The heterochromatin-like complex so targeted nucleates the subsequent "spreading" and formation of a larger domain (Figure 4B). A coarse-grained polymer model of genomic bookmarking predicts, as one of three parameters required for robust epigenetic inheritance of chromatin states, a critical density of bookmarks along a chromatin fibre to be 1 or 10 nucleosomes per 400 nucleosomes (ϕ_c ~0.04; (154)). We have made a rough estimate of the density of nucleation sites within the B4 sub-compartment using the distribution of KAP1 peaks (Figures 5B to D). In the B4 sub-compartment (14,642 Kb) there are conservatively 353 KAP1 peaks, which corresponds to one nucleation site per ~40Kb, i.e., 200 nucleosomes, where 1 nucleosome is 200bp. The base of the peak of enrichment for H3K9me3 and HP1β around the KAP1sites gives the size of the nucleation site at ~6kB (Figure 5D), which is in agreement with previous studies (104, 114). This indicates an approximate density of bookmarks of ~30 nucleosomes per 200 nucleosomes in the B4 sub-compartment, well within the critical density defined by the coarse-grained

polymer model. The second parameter is that bookmarking involves the sequence-specific recruitment of the machinery that epigenetically-modifies chromatin. The KRAB-ZNP that targets the nucleation complex (Figure 4A) satisfies that requirement. The third parameter is the operation of a positive feed-back mechanism that can spread and establish the domain. This too is met because of the self-reinforcing SUV39H1-mediated spreading of H3K9me3 (Figure 4B) that generates the domain from the nucleation site (Figure 4A). The organisation of the KRAB-ZFP heterochromatin-*like* domains therefore satisfies the theoretical requirements for "*epigenetic domains*" (154).

Replication of the heterochromatin-*like* domains/complexes during S-phase has been treated in detail elsewhere (100). Briefly, it involves two complexes called the CAF-1 and SMARCAD1 complexes; both complexes contain KAP1 and HP1 and K9 HTMases that are key components involved in replication of heterochromatin (155–158).

Heterochromatin-like domains/complexes and compartmentalisation

Contacts of heterochromatin-*like* domains/complexes with constitutive heterochromatin are likely to lead to coalescence and promote *macroscopic* PPPS. When heterochromatin-*like* domains/complexes are brought into contact with constitutive heterochromatin, where the latter is enriched in high concentrations in H3K9me3, many HP1-H3K9me3 inter-fibre contacts will be formed (46) (Figure 6A). The domains/complexes will merge with the large blocks of constitutive heterochromatin because their constituents are, by definition, essentially the same (Table 1) and bridging molecules, such as HP1, are unable to distinguish between the translocated domain/complex and the large block of heterochromatin. Cross-linking and merging of the domain/complex with constitutive heterochromatin would contribute to de-mixing and macroscopic phase separation (86, 87) (Figures 5A and 6A) with domains/complexes becoming seamlessly part of μm-sized cytologically-visible constitutive heterochromatin. The ZNF91 KRAB-ZNF cluster that lies within peri-centric heterochromatin (159) undergoes macroscopic phase separation (asterisk in Figure 5A) and its interaction with other peri-centromeric regions and more distal sites will also lead to macrophase separation (ovals with solid lines in Figure 5A). Macrophase separation may also take place with odorant receptor genes that form very large heterochromatin-*like* domains up to 5Mb in size (Table 1), 45–50% of which exhibit a preferential localisation to constitutive heterochromatin in post-mitotic olfactory sensory neurons (160). Other KRAB-ZNF clusters spread out along the arm of chromosome 19 (104) are assembled into heterochromatin-*like* domains where *cis*- contacts between them (ovals with dotted lines in Figure 5A) contribute to the B4 heterochromatic sub-compartment in Hi-C experiments (105).

Heterochromatin-*like* domains along the arms of chromosome 19 that are flanked by stretches of "euchromatic" nucleosomes (Figure 5A) will, we suggest, behave like blocks in a block copolymer (BCP). Polymers that contain blocks of at least two (or more) different types of monomer are called BCPs (161, 162) where a block is made up of identical monomers. BCPs share many of the properties of homo-polymers excepting that the covalent bond connecting the different types of block prevents *macroscopic* phase separation. Instead, BCPs undergo *microscopic* phase separation when one block becomes highly enriched and incompatible resulting in phase separation to form nanostructures in the range of 0.1 to 100 nm (162). For a heterochromatin-*like* "block", enrichment (leading to incompatibility) would result from HP1-mediated bridging of H3K9me2/3-marked nucleosomes *within* the "block" (Figure 6C) and this could drive micro-phase separation (asterisks in Figure 6). *cis*- contacts mediated by HP1 "bridging" *between* micro-phase separated heterochromatin-*like* "blocks" (Figure 6D; ovals with dotted lines in Figure 5A) could explain the emergence of the B4 compartmental domain identified in Hi-C maps (105) (Figure 5A). Specifically, given that: (i) KRAB-ZNF clusters are assembled into heterochromain-*like* domain ("blocks") enriched in H3K9me3 and HP1 (104, 113), (ii), HP1 can act as a "bridge" between H3K9me3-marked nucleosomes (46, 74, 77) and, (iii), HP1 can also act as a bridge between distantly located loci (73, 74), it is unsurprising that the KRAB-ZNF heterochromatin-like domains ("blocks") make far *cis*- contacts that emerge as the B4 sub compartment in Hi-C maps (105). Importantly, treating chromatin fibres as BCPs has been used with considerable success to accurately simulate contact maps derived from Hi-C experiments (154, 163–166).

Heterochromatin-*like* domains/complexes and Hi-C maps

Heterochromatin-*like* domains/complexes (Table 1) are contiguous with the chromatin fibre that is tightly folded within the confines of the nucleus. As part of the fibre, the domains/complexes will fold and experience a myriad of *cis*- and *trans*-chromosomal contacts. Many will be transient and of low frequency. Others will occur more frequently and endure, as will be the case for contacts mediated by HP1-H3K9me2/3 interactions (Figure 6D). A measure of folding can be assessed by Hi-C, a high throughput technique that generates contact frequency (Hi-C) maps (167). Hi-C maps derived from *bulk* populations of cells revealed the first folding paradigm – the well-known checkerboard (or plaid) pattern of contact enrichment (8) (Figure 7A). The pattern is cell-type specific (168, 169) and identifies a set of loci that interact both *in cis* and *trans* between Mb-sized genomic intervals that can be classified on the basis of computational correlation and principal component analysis as either an A or B compartment, where there is higher contact frequency between genomic loci of the same type (A-A and B-B type contacts) and reduced contact frequency between loci of different type (A-B type contacts) (8). Characterisation showed that A-type compartments carry euchromatic marks, are gene rich, transcriptionally active, and early-replicating (170). By contrast, B-type compartments were found to carry heterochromatic marks, are gene poor, late replicating and often associated with the nuclear lamina (170). On

this basis, the checkerboard contact pattern is thought to represent the folding of chromatin into euchromatin (A-type compartments) and heterochromatin (B-type compartments) (8).

Contacts between heterochromatin-*like* domains/complexes should segregate with the B-type heterochromatic compartments. Large domains do. As explained, the B4 heterochromatic sub-compartment contains 130 KRAB-ZNF genes from the clusters on human chromosome 19 that are assembled into heterochromatin-*like* domains (104, 105) (Table 1). However, the checkerboard pattern in Hi-C maps (8, 171) (Figure 7A) does not show signs of the smaller domains/complexes (Table 1). They may now have been observed in Hi-C maps generated from *Nipbl*$^{-/-}$ liver cells where chromatin-associated cohesin was depleted (171) (Figure 7E). This revealed a finer heterochromatic B-type compartmentalisation that *emerged* from the A-type compartments; canonical B-type compartments did not exhibit fragmentation. Notably, loci in the A-type compartments retained their euchromatic epigenetic marks *i.e.*, A-type loci do not turn into B-type loci in *Nipbl*$^{-/-}$ cells. The absence of the finer B-like compartments in wt Hi-C maps is because B-B contacts involving loci within the finer B-type compartments are continuously disrupted by ATP-dependent loop extrusion, whereupon the loci segregate with the A-type compartments. It is only when chromatin-associated cohesin is depleted that those contacts are re-instated and the finer, innate, B-type compartments emerge from the A-type compartments (171).

Cohesin is a loop-extruding factor (LEF) (164, 166). LEFs attach to the chromatin fiber at random positions and reel it in from both sides, thereby extruding a progressively growing chromatin loop (Figure 7, top row) until they either fall off, bump into each other, or bump into extrusion barriers such as CTCF, which define TAD boundaries (164, 166, 171). Loop extrusion is an energy-driven, ATP-dependent, process (172). Based on the known activity of LEFs, a simple explanation for the "masking" of the finer, innate, B-type compartments in wt cells and their emergence from A-type compartments in cohesin-depleted cells can be posited drawing upon polymer physics, where heterochromatin-*like* domains/complexes are treated as one of the blocks in a BCP (162) (Figure 6). The general principles can be illustrated by analytical treatment of a bulk BCP made up of two blocks A and B, where electrostatic interactions are negligible. Micro-phase separation is dependent on three parameters: (i) the volume fraction of the blocks A and B (f_A+f_B=1), (ii) the total degree of polymerisation ($N=N_A+N_B$) and, (iii), the Flory-Huggins parameter, χ_{AB} (173). The χ_{AB}–parameter is key, because it specifies the degree of incompatibility between the A and B blocks and this is what ultimately drives micro-phase separation; a positive χ_{AB}–parameter means the blocks are incompatible and the larger χ_{AB} is the more incompatible they are. The degree of micro-phase separation of the BCP is determined by the segregation product, $\chi_{AB}N$. Given that the incompatibility is significant (*i.e.*, the energy cost of mixing A and B is high; χ_{AB} is positive) and $\chi_{AB}N>10$ the BCP will de-mix and micro-phase separate. Because the χ–parameter varies

inversely with thermal energy an increase in temperature decreases the incompatibility between the constituent blocks and mixing takes place; de-mixing and micro-phase separation resumes upon cooling. In a similar way, LEF-dependent (ATP-consuming) extrusion of a chromatin loop containing a heterochromatin-*like* domain/complex ("block") embedded within euchromatin results in mixing of the domain/complex with euchromatin. Mixing takes place because the energy-driven extrusion disrupts the HP1-mediated "bridging" of H3K9me3-marked nucleosomes (Figure 7C); incompatibility is reduced as the "block" becomes less "heterochromatic" and more "euchromatic". Moreover, because phase separation of BCPs is dependent upon volume fraction, mixing has a greater effect on smaller complexes than larger domains (*c.f.* Figure 7B with 7C). Put simply, mixing of smaller heterochromatin-like complexes with larger regions of surrounding euchromatin during loop extrusion will effectively make loops "homogeneous" with respect to euchromatin. This will promote incorporation of smaller complexes into A-type compartments (see blue arrows in top row of Figure 7). When energy-driven loop extrusion is inhibited by cohesin depletion (analogous to cooling a BCP) HP1 "bridging" of H3K9me2/3-marked nucleosomes within the complexes is reconstituted resulting in de-mixing and micro-phase separation (Figure 7F) as observed for "blocks" in a BCP. Even the smallest heterochromatin-*like* complexes are likely to phase separate; polymer simulations and chromatin fragmentation experiments indicate that the minimal size of a chromatin "block" required for phase separation is around ~10-20kb (163, 174). The newly micro-phase separated complexes ("blocks") can then engage in *cis*- and *trans*- contacts mediated by HP1 "bridging" of H3K9me2/3-marked nucleosomes (Figure 7F and red arrows in bottom row of Figure 7). And it is these contacts that emerge from the A-type compartments as the finer B-type heterochromatic compartments (171). If heterochromatin-*like* domain/complexes throughout the genome are likewise subject to mixing by LEF activity, compartmentalisation detected by Hi-C experiments would be coarser and less well defined in wt cells. This is indeed what is observed when wt and cohesin-depleted Hi-C maps are compared (*c.f.* Figure 7A with 7E) (171).

Conclusions and perspectives

HP1-mediated bridging of H3K9me2/3-marked nucleosomes provides a mechanism that connects epigenetics, PPPS and compartmentalisation. Bridging of H3K9me2/3-marked nucleosomes by HP1 is involved in nucleation and assembly of heterochromatin-*like* domains/complexes that epigenetically regulate chromatin-templated processes (Table 1; Figures 2 to 5). Bridging promotes PPPS, where macro-phase separation takes place in constitutive heterochromatin and micro-phase separation with heterochromatin-*like* domains/complexes (Figures 5A and 6). Contacts that result from HP1-mediated bridging of H3K9me2/3-marked nucleosomes are likely detected in Hi-C maps as loci that fall within B-type compartmental domains (Figure 7). Based on these data testable predictions and explanations can be posited that could provide insight into chromatin-templated processes and genome compartmentalisation. We also redefine B-type

heterochromatic compartmental domains as *epigenetic compartmental domains* that represent the "epigenetic" component of cellular identity.

HP1-mediated bridging of H3K9me2/3 nucleosome fibres and compartmentalisation

Bridging of H3K9me2/3 nucleosome fibres by HP1 proteins is likely to contribute to compartmentalisation detected in Hi-C maps (Figure 7) and to that observed with cytologically-visible constitutive heterochromatin (Figure 6). To test the role of HP1 proteins in compartmentalisation it would necessary to delete all three HP1 proteins in mammalian cells. HP1α/β/γ null ES die around a week after deletion of the genes (unpublished result), but conditional deletion of all three HP1 isotypes has been achieved in bi-potential mouse embryonic liver (BMEL) cells (175). BMEL cells represent a system to test the role of heterochromatin-*like* domains/complexes on compartmentalization seen in Hi-C maps (is there (partial) collapse of B-type compartments in HP1α/β/γ null BMEL cells?) and whether domains/complexes affect LEF-dependent loop extrusion dynamics.

HP1α/β/γ null BMEL cells can also be used to investigate cytologically-visible compartmentalization, specifically the functional relevance of constitutive heterochromatin positioning at the nuclear periphery. In conventional nuclei, constitutive heterochromatin is found at three locations in the interphase nucleus - internally as large domains called chromocenters, adjacent to nucleoli or at the nuclear periphery (176). When peripheral heterochromatin is experimentally untethered it re-localizes from the periphery to the nuclear interior and coalesces with other domains to form a single large phase-separated block of heterochromatin (177, 178). Strikingly, despite the obvious change in nuclear organization, compartmentalization as detected in Hi-C experiments was unchanged (178). This raised the question of what the functional relevance of peripheral heterochromatin is. We suggest that tethering of constitutive heterochromatin to the periphery inhibits aggregation of macro-phase separated constitutive heterochromatin domains into the single large phase separated block that is observed in the "untethered" nuclei (177, 178). The factors that are likely to promote aggregation include molecular crowding (2, 4) and bridging molecules such as HP1 proteins (Figures 2 and 3). The tendency to aggregate can be stopped by tethering constitutive heterochromatin to a larger structure, such as the nuclear lamina. Heterochromatin anchored to the periphery could further resist aggregation of internal heterochromatin domains through fibers that emanate from the periphery to the internal domains. A prediction of this simple model is that the chromatin fibers connecting the periphery to the internal domains are "spring-loaded" and deletion of HP1 proteins, which removes one of the forces driving aggregation, would lead to movement of the internal domains towards the periphery as the fibres relax. This is, in fact, what is observed in HP1α/β/γ null BMEL cells (Figure 3D in (175)). HP1α/β/γ null BMEL nuclei also show a reduction in H3K9me3, albeit

many nuclei still possess dense constitutively heterochromatic domains –mostly located at the periphery - indicating that other interactions, in addition to the HP1-H3K9me3 interaction, are involved in macro-phase separation of constitutive heterochromatin. As explained, these could include, *inter alia*, other bridging molecules (3) or an affinity between homotypic DNA repetitive elements (95).

There are examples in nature where aggregation of heterochromatin into a single mass is programmed as part of normal development. In nocturnal mammals rod photoreceptors have non-conventional nuclei where heterochromatin aggregates into a single internally-located block, which acts as a micro-lens to facilitate nocturnal vision (179). Here, aggregation is an advantage; the process of *maturation* or *hardening* of the phase-separated block could, moreover, lead to formation of a more solid glassy/liquid crystalline phase (63) that might possess lens-like properties. Such being the case, natural selection will have seen to it that peripheral heterochromatin was untethered from the nuclear lamina in rod photoreceptors. This is what appears to have happened (177, 179).

Heterochromatin-like domains/complexes and self-assembly of BCPs

Micro-phase separation of block copolymers in solution can result in self-assembly into a wide variety of nano-structures (180), including vesicles, rods and liquid-crystalline lamellae (181). The ability of heterochromatin-*like* domains/complexes to likewise adopt different micro-phases will influence their properties and function. For example, heterochromatin-*like* domains/complexes that behave as liquid crystals (182) provide an explanation for heterochromatic PEV, where a heterochromatic gene variegates when placed in a euchromatic environment (183). A liquid-crystalline micro-phase could be promoted by the atypical organisation of heterochromatic genes, where their introns are replete with middle repetitive sequences similar to those located in regions of peri-centric heterochromatin (184). Viewing domains/complexes as liquid crystals might also provide an explanation for the proximity effects (182) seen with variegating heterochromatic genes (185), and the sole example of dominant PEV, *brown-dominant* (bw^D) variegation (186).

Heterochromatin-like domains/complexes and the phylotypic stage of vertebrate development

The phylotypic stage of vertebrate development represents the archetype of the basic body plan, where there is high morphogenetic similarity between different vertebrate species (187–189). This stage represents the "bottle-neck" in the hour-glass model of development, where embryos exhibit greater variation at the earliest stages and at later stages but at the phylotypic stage there is an evolutionary restriction ("bottle-neck") in which only a reduced amount of evolution is allowed and, as a consequence, the morphologies of the embryos are similar (190). It is unclear how this mid-embryogenesis stage of development has come to be the most conserved but it is thought to involve the activity of conserved transcription/chromatin factors and

developmental signaling pathways, where perturbations in these mechanisms have fatal consequences, thus leading to evolutionary conservation (191, 192). Recent work has shown that H3K9me3-marked heterochromatin is deployed transiently in germ layer cells – overlapping with the phylotypic stage - to repress genes associated with fully-differentiated cell function and then, as development proceeds, to undergo reorganization and loss during lineage specification (110, 193). Assembly of differentiation-specific genes into H3K9me3-marked heterochromatin may represent one of the conserved chromatin-based mechanisms that regulate the "phylotypic restriction". It is tempting to speculate that the H3K9me3-marked heterochromatin assembled in germ layer cells may contain heterochromatin-*like* domains/complexes (Table 1) and like the domains/complexes is subject to HP1 "bridging" and PPPS (Figure 6).

PPPS of H3K9me3-marked heterochromatin could explain its resistance to sonication after chemical cross-linking (109). Sonication resistant heterochromatin (srHC) has been isolated from human fibroblasts and sequenced (109, 193) and shown to contain the B4 sub-compartment (Figures 5B and C). We have found that the 1.2Mb superTAD, which contains >70 genes at the clustered Protocadherin (cPcdh) locus (Table 1) (106) is also found in srHC (109). The cPcdh exons are expressed combinatorially in neurons and the Protocadherin proteins that arise from this process form multimers that interact homophilically and mediate a variety of developmental processes, including neuronal survival, synaptic maintenance, axonal tiling, and dendritic self-avoidance (194). The Protocadherin superTAD is regulated by the KRAB-ZNP pathway and, notably, ablation of the SETDB1 H3K9HMTase leads to collapse of the entire superTAD (106). It will be of interest to investigate whether srHC isolated from germ layer cells contain other KRAB-ZNP-regulated TADs and compartments. This would indicate a role for KRAB-ZNPs and the heterochromatin-*like* domain/complexes they assemble in regulating the "phylotypic restriction" during vertebrate development.

"Epigenetic compartmental domains" (ECDs) and the regulation of cellular identity

At the outset it was posited that the HP1-containing heterochromatin-*like* domains/complexes would be mechanistically related to Polycomb (Pc)-containing domains/complexes (99, 195, 196). The similarity between HP1- and *Pc*-domains/complexes extends to their ability to phase separate and to generate B-type heterochromatic compartmental domains in Hi-C maps. For one, the mammalian *Pc* homologue CBX2, like HP1 proteins, can promote phase separation that is dependent upon amino-acids in CBX2 necessary for nucleosome fibre compaction (197, 198). Second, the histone modifications H3K9me2/3 and H3K27me3 are diagnostic for HP1- and *Pc*-dependent domains/complexes respectively (Table 1) (199) and are used, *inter alia*, to define B-type compartmental domains (170). Given that H3K9me2/3 and H3K27me3 are the only histone modifications that are truly epigenetic (199) we suggest that the B-type compartmental domains generated by HP1- and Pc- dependent domains/complexes are *epigenetic compartmental domains* (ECDs) that drive the

compartmentalisation seen in Hi-C maps in the same way that cytologically-visible compartmental segregation is driven *solely* by heterochromatin (178).

ECDs could have functional significance. ECDs may represent the "epigenetic" component of cellular identity where the other component, tissue-specific gene expression, is represented by contacts that generate the euchromatic A-type compartments. In this way, compartmentalisation observed in Hi-C maps decouples epigenetics from tissue-specific gene expression. There is evidence that supports a role for HP1 proteins in regulating the "epigenetic" component of cellular identity. It comes from studies on mammalian HP1β, which mediates contacts between H3K9me2/3-marked nucleosomes (Figure 2; (46)) and thus likely to contribute to ECDs. HP1β is necessary for maintaining pluripotency of ES cells and the differentiated state of fibroblasts (200). The cellular identities of two different cell types expressing divergent patterns of gene expression are both safeguarded by HP1β. In the absence of HP1β cellular identity becomes unstable. It would seem that perturbation of contacts between heterochromatin-*like* domains/complexes might increase cellular plasticity of differentiated cells, which should in turn enhance their reprogrammability by iPS reprogramming factors. In this regard, RNAi screens for genes whose inhibition enhance reprogramming efficiency identified genes encoding CAF-1, the SUMO-conjugating enzyme UBE2i, SUMO2, SETDB1, ATRX and DAXX proteins (111, 112). Strikingly, all are involved in either nucleation or replication of heterochromatin-*like* domains/complexes (Table 1; Figures 1G and 4A; (100)). A prediction would be that RNAi-inhibition of these genes would perturb ECDs in Hi-C experiments. This remains to be tested.

Author contributions

PBS conceived of the synthesis presented and wrote the first draft. AGN undertook the bio-informatic analyses and drew the figures. Both authors revised and approved the final manuscript.

Author details
1Nazarbayev University School of Medicine, 5/1 Kerei, Zhanibek Khandar Street, Nur-Sultan Z05K4F4, Kazakhstan.
2Epigenetics Laboratory, Department of Natural Sciences, Novosibirsk State University, Pirogov Str. 2, Novosibirsk 630090, Russian Federation.
3Institute of Cell and Neurobiology, Charité – Universitätsmedizin Berlin, Corporate member of Freie Universität Berlin, Humboldt-Universität zu Berlin, and Berlin Institute of Health, Berlin, Germany.

Acknowledgements
Not applicable.

Competing interests
The authors declare that they have no competing interests.

Availability of data and materials
Bioinformatic methods:
Co-ordinates for genes within the B4 sub-compartment annotation was obtained using the UCSC table browser, which was then reduced to unique positions using simple shell commands. Reads from ChIPseq were trimmed for quality using Trimmomatic SE and aligned to GRCh37/hg19 using Bowtie2 (201). KAP1 peaks were called using MACS. Read coverage was normalized to reads per genomic context (1X), input-subtracted and plotted using deeptools (202). The entire pipeline was deployed using Snakemake (203). Genomic coverage was visualized using the IGV genome browser. The Reprogramming Resistant Regions (RRRs) annotation was graciously provided by Dr. Yi Zhang, which was converted to human coordinates using the UCSC's liftover tool. Hi-C contact frequency map for chromosome 19 in H1-ESCs was obtained by using the 3D genome browser (204).

Data	**Publication**	**GEO Acc.**
Input Subtracted H3K9me3 ChIP from euchromatin and Sonication-Resistant Heterochromatin	Becker et al 2017 PMID: 29272703	GSE87041
HP1β & Control ChIP in HEK293	LeRoy et al., 2012 PMID: 22897906	GSE39579
H3K9me3 & KAP1 ChIP & Input in naïve ES cells	Theunissen et al., 2017 PMID: 27424783	GSE84382
B4 subcompartment Annotation (modified to include chr19:19,775,198-24,317,418 - Vogel et al., 2006)	Rao et al., 2014 PMID:25497547	GSE63525
Hi-C Contact Map in H1-ESCs	Dixon et al., 2015 PMID:25693564	GSE52457

Consent for publication
Not applicable.

Ethics approval and consent to participate
Not applicable.

Funding
This work was supported by a grant from the Ministry of Education and Science of Russian Federation #14.Y26.31.0024; PBS was also supported by Nazarbayev University Grant 090118FD5311.

Figure Legends:

Figure 1: Structure-function relationships of mammalian HP1β. Depicted are the functional properties of the HP1β domains, its interaction with H3K9me3 and the PxVxL penta-peptide motif. (**A**) Cartoon summarizing the functional properties (left) and interactions of different domains of hHP1β (right). The specificity of HP1β CD interaction with H3K9me3-marked chromatin can be modulated by the negatively and positively charged residues within the NTE and HR (46). (**B**) The HP1β CD (PDB code 1GUW) forms a three-stranded β-pleated sheet that abuts to a α-helix. The site of the shallow groove to which the H3-tail binds is between the third strand, a C-terminally adjacent coil segment and the N-terminal segment [Note: this conformation corresponds to the peptide bound complex]. (**C**) The HP1β CD (1GUW; cyan) complexed with the H3K9me3 tail peptide (1KNA; yellow stick) superimposed on the HP1β CD alone (1AP0; grey). Binding of the H3K9me3 tail peptide causes the CD N-terminal region to draw upward and wrap around the peptide. meK9: methyl-ammonium group. (**D**) A consequence of this induced fit is that a notional aromatic 'cage' is formed from three conserved aromatic residues: Tyr21, Trp42 and Phe45. The interaction between the methyl-ammonium moiety and the aromatic cage is largely electrostatic and mediated by cation-π interactions where the positively charged (cation) moiety is attracted to the negative electrostatic potential of the aromatic groups' π-system (36). (**E**) The HP1β CSD monomeric subunit (PDB code 1SZ4) (38) shows a similar mixed α/β fold as the HP1β CD, except for an additional α-helix that is shown facing the reader. The CSD has a groove corresponding to that found in the CD, but is partly occluded (in the vicinity of the putative K9 binding site) by the N-terminal residues of the CSD. (**F**) Structure of the HP1β CSD dimer (1SZ4). The monomers have an affinity of K_D ~150 nM; homodimer formation mainly involves interactions between the α2 helices. The dimer creates a groove between the first β-strand and the C-terminal segment at the CSD–CSD interface which can bind proteins that possess the PxVxL motif (38, 39). (**G**) Surface view of the CSD homodimer (one monomer in pink and the other in blue) bound to the CAF-1 peptide (shown as a stick model) containing the PxVxL motif, which is involved in intermolecular β pairing with both monomers (38). Figure (**A**) was modified from (46). (**B**) to (**G**), with legend, were taken from (59).

Figure 2: Bridging of two nucleosomes by HP1 as seen in the structure of the HP1α/β/γ-dinucleosome complex. In **(A)** three orthogonal views of the reconstructed three-dimensional structure of HP1α-dinucleosome complex. A model of the nucleosome core particle (PDB code 3LZ0) is docked into each of the two nucleosome densities. The linker DNA and the bridging HP1α dimer are clearly distinguishable and the linker does not interact with the HP1α dimer. Scale bar, 10A°. In **(B)** to **(D) t**he HP1α-dinucleosome complex **(B)**, the HP1β-dinucleosome complex **(C)**, and the HP1γ-di-nucleosome complex **(D)** are shown. In **(E)** all three HP1-

dinucleosome complexes are superimposed, where the HP1α-dinucleosome complex is in grey, the HP1β-dinucleosome complex is in orange and the HP1γ-dinucleosome complex is in green. The orientations of the left nucleosomes are fixed. Taken from (77).

Figure 3: A schematic model for how HP1 bridging of H3K9me2/3-marked nucleosomes drives PPPS of constitutive heterochromatin. "Clutches" (smaller, darker, blue ovals) of H3K9me2/3-marked nucleosomes (red spheres) organized in an irregular zig-zag structure where linker length is variable. Given the zig-zag organization, HP1 proteins preferentially "bridge" nucleosomes that are second nearest neighbors in the zig-zag rather than closest neighbors thereby stabilizing the zig-zag geometry (top inset on right). There is also bridging between "clutches" (middle inset on right) that could, in addition to osmotic depletion attraction, result in merging of "clutches" into larger ordered globules (larger, lighter, blue ovals). Further bridging between globules (bottom inset on right) could lead to formation of self-similar larger globules. These may then form even larger globules ("globules of globules"; not shown) (8). Bridging of H3K9me2/3-marked nucleosomes by HP1 proteins into these different condensed structures in heterochromatin contributes to PPPS of constitutive heterochromatin. The dark "dots" represent molecular species that contribute to the entropic molecular crowding effect that promotes merging.

Figure 4: Nucleation and spreading of a KRAB-ZNF heterochromatin-*like* domain. In (**A**) is the heterochromatin-*like* complex that is assembled at the 3' end of KRAB-ZNF genes. These complexes nucleate the KRAB-ZNF heterochromatin-*like* domains that encompass the KRAB-ZNF gene clusters. The diagram is based on the KAP1 and HP1 interactomes. (**1**) The KRAB-ZNP binds to its DNA binding site through its zinc-fingers (Zn). **(2**) The KRAB domain of the KARB-ZFP interacts with the RBCC domain of KAP1 (121). The structure of KAP1 is taken from (205). A HP1 CSD dimer binds to one molecule of KAP1 through the PxVxL motif (the HP1-box). The HP1 CD binds to H3K9me3. (**3**) The PHD domain of KAP1 is an E3 ligase that co-operates with UBE2i to sumoylate the KAP1 bromodomain (125, 126). (**4**) The sumoylated bromodomain is bound by the NuRD complex that deacetylates acetylated histones (green circle) in preparation for histone methylation (136). (**5**) SETDB1 H3K9 HMTase interacts with the sumoylated bromodomain (125) and generates H3K9me3 (orange circles). (**6**) The ATRX/DAXX complex is bound to KAP1, HP1, and H3K9me3. ATRX/DAXX incorporates replacement histone H3.3 into chromatin thereby reinforcing nucleation (133). (**7**) HP1 recruits a H4K20 HMTase that generates H4K20me3 (orange circles). This is the H3K9me3:HP1:H4K20me3pathway. (**8**) The maintenance DNA methylase DNMT1 binds to KAP1 (143, 144). Np95 is the co-factor of DNMT1 and is also recruited by KAP1 (142). DNMT1 maintains cytosine methylation at the site of assembly (143, 144). Not shown are the de novo DNMTases, DNMT3A and DNMT3B, which can interact with KAP1 (143, 144). It is known that the H3K9me3 and HP1 enrichment at the 3' end of the KRAB-

ZNF genes extend ~6kB at the site of assembly of the nucleation complex (104, 114) (Table 1). Taken and modified from (100). In (**B**) is a coarse-grained model depicting SUV39H1-mediated spreading of H3K9me3 and HP1 proteins that form the larger KRAB-ZNF domain. In top left hand panel depicts the nucleation complex (shown in **A**) generating H3K9me3-marked nucleosomes (red filled circles) in "clutches" on either side of the complex. The top right-hand panel shows the CD of SUV39H1 attaching to H3K9me3-marked nucleosome within a clutch whereupon the SUV39H1 SET domain catalyzes the SAM-dependent methylation of H3K9, which therefore provides a positive feedback loop (147) that enables spreading of the domain in the 5' direction away from the nucleation site (114). In bottom left hand panel SUV39H1 is depicted as mediating "looping-driven" spreading of H3K9me3 (red arrow), where spreading is not restricted to next-neighbour interactions but can skip nucleosomes, as it does here where one "clutch" is "looped-out" and whose constituent nucleosomes are not methylated at H3K9. This is likely to be relevant to the KRAB-ZNF genes which show a depletion of H3K9me3 and HP1β at their 5' ends (104, 114). In the wake of the newly-deposited H3K9me3 HP1 dimers bind H3K9me3 through their CDs. The bottom right-hand panel depicts continued spreading of H3K9me3 by SUV39H1 activity (red arrow) and HP1-mediated bridging of H3K9me3-marked nucleosomes within and between "clutches". Bridging results in chromatin compaction.

Figure 5: The B4 sub-compartment and the density of nucleation sites within the sub-compartment. (**A**) Shows the contact frequency map in H1-ESCs from which the B4 sub-compartment emerges. The B4 sub-compartment (annotation combined from (104) and (105)) overlaps exactly with regions enriched for HP1β, KAP1 and H3K9me3, which are given below the chromosomal map. Increased contact frequency can be observed within peri-centric regions, such as that marked with the asterisk (*), which denotes a large pericentric KRAB-ZNF cluster that likely undergoes macro-phase separation (see Figure 6 and text for details). Contacts between the peri-centric KRAB-ZNF cluster and other peri/centric regions and more distal sites (ovals demarked by solid lines) are also likely to undergo marco-phase separation. Also shown are contact enrichments between non-pericentric B4 sub-compartments (ovals with dotted lines) that likely represent contacts between micro-phase separated HP1-containing block co-polymers (see Figure 6 and text for details). The magnifications in (**B**) and (**C**) illustrate the overlap of the B4 compartment with KAP1/H3K9me3/HP1β in more detail. Nucleation sites, as defined by KAP1 peaks, occur at a frequency of 1 every ~40kbp over the B4 sub-compartment. (**D**) Depicts the profile of KAP1, H3K9me3 and HP1β binding at the 3' end of KRAB-ZNF genes, anchored by the Transcription End Site (TES). The KAP1 peaks are on average 1kbp in width and surrounded by HP1 and H3K9me3 enrichment that extend ~6kb. (**B**) and (**C**) also show the distribution of H3K9me3 and sonication resistant heterochromatin (srHC) within the B4 sub-compartment, which overlap with the other peaks. Tracks in (**B**) and (**C**) are input-subtracted ChIP of HP1β in HEK293, KAP1 in H1 ES cells, H3K9me3 in H1 ES cells,

H3K9me3 from BJ1 cells, and H3K9me3 from BJ1 srHC respectively. Average coverage in (**D**) is input-subtracted ChIP reads per genomic context (RPGC) per 1000bp bin.

Figure 6: *Macro*- and *micro*-phase separation of heterochromatin-*like* domains/complexes. To the left of the figure constitutive heterochromatin is depicted as ordered globules, ranging from smaller to larger. (**A**) depicts "clutches" that contain H3K9me2/3-marked nucleosomes (red spheres) organized in an irregular two-start zig-zag organization. Within the "clutches" HP1 proteins preferentially "bridge" nucleosomes that are second nearest neighbors in the zig-zag rather than closest neighbors thereby stabilizing the zig-zag geometry. HP1 proteins also act as bridges within and between "clutches" and "globules" Also shown in (**A**) is a heterochromatin-*like* domain consisting of "clutches" of HP1-bridged H3K9me2/3-marked nucleosomes (red spheres) that runs alongside constitutive heterochromatin. When brought into close apposition to constitutive heterochromatin, an environment rich in HP1 and H3K9me3, extensive cross-linking of the heterochromatin-*like* domain to constitutive heterochromatin takes place mediated by HP1 proteins. This contributes to *macro*-phase separation, where the heterochromatin-*like* domain merges with cytological-visible constitutive heterochromatin. The same heterochromatic fibre extends to the right into the nucleoplasm away from constitutive heterochromatin and joins a euchromatic segment consisting of "clutches" containing "euchromatic" nucleosomes (blue spheres in (**B**)) that exhibit less of the two-start contact geometry of H3K9me2/3-marked nucleosomes but rather possess a more disordered or heterogeneous organization. The "euchromatic" fibre in turn extends into a heterochromatin-like domain/complex consisting of "clutches" containing HP1-bridged H3K9me2/3-marked nucleosomes, as shown in (**C**). HP1-mediated bridging of H3K9me3-marked nucleosomes leads to enrichment of both and promotes *micro*-phase separation that is characteristic of block copolymers (see text for details). "Blocks" of heterochromatin-*like* domains/complexes can engage in *cis*- (shown in (**D**)) and *trans*- interactions (now shown). *Cis*-interactions, as shown in (**D**), could explain the emergence of the B4 sub-compartment from contacts between the KRAB-ZNF heterochromatin-*like* domains on human chromosome 19.

Figure 7: Heterochromatin-*like* domain/complexes and the emergence of finer compartmental domains in *Nipbl*$^{-/-}$ cells. In (**A)** is a cartoon representation of a wild-type Hi-C pattern of interphase chromatin organization. The strength of each pixel indicates the relative pairwise contact probability of two-loci. Along the diagonal are squares of increased contact frequency that represent TADs. The off-diagonal checkerboard pattern represents compartmentalization. To the right of (**A)** is a mechanistic model of how contacts between heterochromatin-*like* domains/complexes contribute to the compartmentalization in wt cells (depicted in (**A**)). There are three loops (labelled 1, 2 and 3) that form due to LEF-driven (ATP-dependent) loop extrusion (LEFs are given as yellow ovals; extrusion given by black arrows). Loop 1 is a homo-polymer entirely composed of "clutches" of H3K9me2/3-marked nucleosomes (given as red circles) that are organized as two-start helix, where the second-

nearest nucleosomes are preferentially bridged by HP1 proteins; there is also bridging between clutches (depicted in **B**). As loop 1 is extruded by the LEFs there is some disruption of the HP1-mediated bridging of H3K9me2/3-marked nucleosomes within and between the "clutches" (as depicted by the unbound HP1 dimers surrounding the LEFs) but the size and homogeneity of loop 1 makes the HP1 bridging largely resistant to disruption by ATP-driven loop extrusion. Loop 1 will make contacts with (far) *cis*- and *trans*-loci (red arrow) that will be seen as an increase in contact probability in B-type heterochromatic compartments. Loop 1 is connected to loop 2 *via* "clutches" of "euchromatic" nucleosomes (given a blue circles) that exhibit less of the two-start contact geometry of H3K9me2/3-marked nucleosomes and possess a more disordered or heterogeneous organization (depicted in (**D**)). Loops 2 and 3 contain smaller heterochromatin-*like* complexes that behave like small blocks in a block co-polymer. Due to LEF-driven (ATP-dependent) loop extrusion the HP1-mediated bridging of H3K9me2/3-marked nucleosomes within and between the "clutches" of the smaller complexes are disrupted (*c.f.* (**C**) with (**B**)). The H3K9me2/3-marked "clutches" take on the character of the "euchromatic" clutches, where the constituent nucleosomes are not bound by HP1 and have a more disordered conformation, as seen in (**C**) . In polymer physics theory the block co-polymer (loops 2 and 3) will have said to have undergone mixing and become "homogenous" with respect to euchromatin. As a consequence, both loops 2 and 3 will be dominated by far *cis*- and *trans*-contacts with A-type loci (blue arrows), which will be seen as an increase in contact probability in A-type compartments; loci within the small heterochromatin-like complexes will now fall into A-type compartments. .

In (**E**) is a cartoon representation of the Hi-C pattern after depletion of the LEF cohesin in *Nipbl*$^{-/-}$ cells [171]. The TADs disappear and a fine-scale compartmentalization emerges that is more defined compared to the wt situation (*c.f.* (**E**) with (**A**)). To the right of (**E**) is a mechanistic model that depicts how contacts between heterochromatin-*like* domains/complexes contribute to the finer compartmentalization in *Nipbl*$^{-/-}$ cells (depicted in (**E**)). The same three loops (labelled 1, 2 and 3) as in the top row, but LEF-driven (ATP-dependent) loop extrusion is absent. This has little effect on the organization of loop 1, which is a homo-polymer made of "clutches" containing of H3K9me2/3 marked nucleosomes that are bridged by HP1 (depicted in (**B**)). The effect of cohesin depletion on the smaller heterochromatin-*like* complexes in loops 2 and 3 is the key to understanding the finer compartmentalization observed. In the absence of cohesin, the energy-driven disruption of HP1-mediated bridging of H3K9me2/3-marked nucleosomes is stopped and the smaller heterochromatin-like complexes are reconstituted (*c.f.* (**F**) with (**C**)). The newly-reconstituted heterochromatin-like complexes de-mix and phase separate as observed for block co-polymers. In (**F**) *cis*-interactions between the larger heterochromatin-like domain (loop 1) and the two newly reconstituted complexes ("blocks"; from loops 2 and 3) are shown. These contacts will be detected in Hi-C experiments as the finer B-type compartments that emerge from the A-type compartments. The red arrows represent potential far cis- and trans-interactions of HP1-bridged

H3K9me3-marked nucleosomes. The blue arrows represent potential far cis- and trans-interaction of "euchromatic" nucleosomes. Figures (**A**) and (**E**) are taken and modified from (164).

Abbreviations:

ADD, ATRX-DNMT3-DNMT3L domain; ATRX, Alpha Thalassemia/Mental Retardation Syndrome X-Linked; BCP, block copolymer; BMEL, bi-potential mouse embryonic liver; CAF-1, chromatin assembly factor 1; *Cbx1, 3, 5*, *Chromobox* homologue *1*, *3* and *5* encoding HP1β, γ and α proteins respectively; CD, chromodomain; CSD, chromo shadow domain; cPcdh, clustered Protocadherin; CTCF, CCCTC-binding factor; DamID, DNA adenine methyltransferase identification; DAXX, Death Domain associated protein; DNMTases, DNA methyltransferases; DNMT1, maintenance DNA methyltransferase 1; DNMT3A, *de novo* DNA methyltransferase 3A; DNMT3B, de novo DNA methyltransferase 3B; DNMT3L, DNA methyltransferase 3L; ECD, epigenetic compartmental domain; ES, embryonic stem; FISH, fluorescent *in situ* hybridisation; FRAP, fluorescent recovery after photo-bleaching; G9a, G9a K9H3 HMTase; GLP, G9a-like K9H3 HMTase; gDMRs, germline differentially methylated regions; H3K9me2/3, *di/tri*-methylated lysine 9 on histone H3; H3K27me3, *tri*-methylated lysine 27 on histone H3; H4K20me3, tri-methylated lysine 20 on histone H4; HMTases, histone methyltransferases; HDACs, histone deacetylases; HR, hinge region; HP1, Heterochromatin Protein 1; iPS, induced pluripotent stem cell; *I(s)*, interaction probability; KAP1, KRAB-associated protein 1; Kb, kilobases; KRAB-ZNPs, k_B Boltzmann's constant; Krüppel-associated box (KRAB) domain zinc-finger proteins; KRAB-ZNF, KRAB domain-zinc finger; KRIP1, KRAB-A Interacting Protein-1; *lacO*, lac operator; lacI protein (encoded by *lacR* gene), inhibitor of the lactose operon; LLPS, liquid-liquid phase separation; LEFs, loop extrusion factors; Mb, megabases; Np95, Nuclear protein 95; NuRD, Nucleosome Remodelling histone Deacetylase; PEV, position-effect variegation; PHD, plant homeodomain; pLI, loss of function intolerance; Pc, Polycomb; PPPS, polymer-polymer phase separation; PxVxL, Proline/Any/Valine/Any/Leucine pentapeptide motif; RBCC, Ring-finger B Box-Coiled Coil domain; RRR, reprogramming resistant regions; SCNT, somatic cell nuclear transfer; SETDB1, SET Domain Bifurcated 1 K9H3 HMTase; siRNA, small interfering RNA; SMARCAD1, SWI/SNF-Related, Matrix-Associated Actin- Dependent Regulator of Chromatin, Subfamily A, Containing DEAD/H Box 1; srHC, sonication resistant heterochromatin; SUMO2, Small ubiquitin-related modifier 2; SUV39H1/2, mammalian Suvar K9H3 HMTase 1 and 2; T, temperature; T_H1, type 1 T helper cell; T_H2, type 2 T helper cell; TAD, topologically-associated domain; Tif1β, Transcriptional Intermediary Factor 1-β; TRIM28, Tripartite motif-containing 28; UBE2i, Ubiquitin conjugating enzyme 2i; wt, wild-type; χ, the Flory-Huggins parameter; Zscan4, Zinc Finger and SCAN domain-containing 4.

References:

1. E. Heitz, *Das heterochromatin der moose* (Bornträger, 1928).

2. A. Bancaud, *et al.*, Molecular crowding affects diffusion and binding of nuclear proteins in heterochromatin and reveals the fractal organization of chromatin. *The EMBO journal* **28**, 3785–3798 (2009).

3. K. Müller-Ott, *et al.*, Specificity, propagation, and memory of pericentric heterochromatin. *Molecular systems biology* **10** (2014).

4. R. Imai, *et al.*, Density imaging of heterochromatin in live cells using orientation-independent-DIC microscopy. *Molecular biology of the cell* **28**, 3349–3359 (2017).

5. V. I. Risca, S. K. Denny, A. F. Straight, W. J. Greenleaf, Variable chromatin structure revealed by in situ spatially correlated DNA cleavage mapping. *Nature* **541**, 237 (2017).

6. M. A. Ricci, C. Manzo, M. F. García-Parajo, M. Lakadamyali, M. P. Cosma, Chromatin fibers are formed by heterogeneous groups of nucleosomes in vivo. *Cell* **160**, 1145–1158 (2015).

7. I. Oh, S. Choi, Y. Jung, J. S. Kim, Entropic effect of macromolecular crowding enhances binding between nucleosome clutches in heterochromatin, but not in euchromatin. *Scientific reports* **8**, 5469 (2018).

8. E. Lieberman-Aiden, *et al.*, Comprehensive mapping of long-range interactions reveals folding principles of the human genome. *science* **326**, 289–293 (2009).

9. J. Langowski, Chromosome conformation by crosslinking: polymer physics matters. *Nucleus* **1**, 37–39 (2010).

10. A. N. Boettiger, *et al.*, Super-resolution imaging reveals distinct chromatin folding for different epigenetic states. *Nature* **529**, 418 (2016).

11. H. J. Muller, Types of visible variations induced by X-rays in Drosophila. *Journal of Genetics* **22** (1930).

12. E. B. Lewis, “The phenomenon of position effect” in *Advances in Genetics*, (Elsevier, 1950), pp. 73–115.

13. J. B. Spofford, Position-effect variegation in Drosophila. *The genetics and biology of Drosophila* **1**, 955–1018 (1976).

14. T. Grigliattia, “Position-effect variegation—an assay for nonhistone chromosomal proteins and chromatin assembly and modifying factors” in *Methods in Cell Biology*, (Elsevier, 1991), pp. 587–627.

15. S. C. Elgin, G. Reuter, Position-effect variegation, heterochromatin formation, and gene silencing in Drosophila. *Cold Spring Harbor perspectives in biology* **5**, a017780 (2013).

16. G. Wang, *et al.*, Conservation of heterochromatin protein 1 function. *Molecular and cellular biology* **20**, 6970–6983 (2000).

17. S. C. Elgin, S. I. Grewal, Heterochromatin: silence is golden. *Current Biology* **13**, R895–R898 (2003).

18. I. J. Hartmann-Goldstein, On the relationship between heterochromatization and variegation in Drosophila, with special reference to temperature sensitive periods. *Genetics Research* **10**, 143–159 (1967).

19. I. F. Zhimulev, E. S. Belyaeva, O. V. Fomina, M. O. Protopopov, V. N. Bolshakov, Cytogenetic and molecular aspects of position effect variegation in Drosophila melanogaster. *Chromosoma* **94**, 492–504 (1986).

20. T. Rudolph, *et al.*, Heterochromatin formation in Drosophila is initiated through active removal of H3K4 methylation by the LSD1 homolog SU (VAR) 3-3. *Molecular cell* **26**, 103–115 (2007).

21. J. Schultz, The relation of the heterochromatic chromosome regions to the nucleic acids of the cell in *Cold Spring Harbor Symposia on Quantitative Biology*, (Cold Spring Harbor Laboratory Press, 1956), pp. 307–328.

22. W. K. Baker, "Position-effect variegation" in *Advances in Genetics*, (Elsevier, 1968), pp. 133–169.

23. C. H. Waddington, The epigenotype. *Endeavour* **1**, 18–20 (1942).

24. P. B. Singh, T. C. James, Chromobox genes and the molecular mechanisms of cellular determination in *Nobel Symposium, Stockholm*, (1995), pp. 71–108.

25. T. Jenuwein, C. D. Allis, Translating the histone code. *Science* **293**, 1074–1080 (2001).

26. A. G. Larson, *et al.*, Liquid droplet formation by HP1α suggests a role for phase separation in heterochromatin. *Nature* **547**, 236–240 (2017).

27. A. G. Larson, G. J. Narlikar, The role of phase separation in heterochromatin formation, function, and regulation. *Biochemistry* **57**, 2540–2548 (2018).

28. B. E. Ackermann, G. T. Debelouchina, Heterochromatin protein HP1α gelation dynamics revealed by solid-state NMR spectroscopy. *Angewandte Chemie* **131**, 6366–6371 (2019).

29. D. O. Jones, I. G. Cowell, P. B. Singh, Mammalian chromodomain proteins: their role in genome organisation and expression. *Bioessays* **22**, 124–137 (2000).

30. E. Minc, Y. Allory, H. J. Worman, J.-C. Courvalin, B. Buendia, Localization and phosphorylation of HP1 proteins during the cell cycle in mammalian cells. *Chromosoma* **108**, 220–234 (1999).

31. P. B. Singh, S. D. Georgatos, HP1: facts, open questions, and speculation. *Journal of structural biology* **140**, 10–16 (2002).

32. A. J. Bannister, *et al.*, Selective recognition of methylated lysine 9 on histone H3 by the HP1 chromo domain. *Nature* **410**, 120–124 (2001).

33. M. Lachner, D. O'Carroll, S. Rea, K. Mechtler, T. Jenuwein, Methylation of histone H3 lysine 9 creates a binding site for HP1 proteins. *Nature* **410**, 116–120 (2001).

34. J. Nakayama, J. C. Rice, B. D. Strahl, C. D. Allis, S. I. Grewal, Role of histone H3 lysine 9 methylation in epigenetic control of heterochromatin assembly. *Science* **292**, 110–113 (2001).

35. P. R. Nielsen, *et al.*, Structure of the HP1 chromodomain bound to histone H3 methylated at lysine 9. *Nature* **416**, 103 (2002).

36. S. A. Baril, *et al.*, Investigation of Trimethyllysine Binding by the HP1 Chromodomain via Unnatural Amino Acid Mutagenesis. *Journal of the American Chemical Society* **139**, 17253–17256 (2017).

37. J. F. Smothers, S. Henikoff, The HP1 chromo shadow domain binds a consensus peptide pentamer. *Current Biology* **10**, 27–30 (2000).

38. A. Thiru, *et al.*, Structural basis of HP1/PXVXL motif peptide interactions and HP1 localisation to heterochromatin. *The EMBO journal* **23**, 489–499 (2004).

39. Y. Huang, M. Myers, R. Xu, Crystal Structure of the HP1-EMSY Complex Reveals an Unusual Mode of HP1 Binding. *Structure* **14**, 703–712 (2006).

40. A. L. Nielsen, *et al.*, Heterochromatin formation in mammalian cells: interaction between histones and HP1 proteins. *Molecular cell* **7**, 729–739 (2001).

41. M. Lavigne, *et al.*, Interaction of HP1 and Brg1/Brm with the Globular Domain of Histone H3 Is Required for HP1-Mediated Repression. *PLoS Genetics* **5**, e1000769 (2009).

42. A. N. Richart, C. I. Brunner, K. Stott, N. V. Murzina, J. O. Thomas, Characterization of chromoshadow domain-mediated binding of heterochromatin protein 1α (HP1α) to histone H3. *Journal of Biological Chemistry* **287**, 18730–18737 (2012).

43. C. Maison, *et al.*, Higher-order structure in pericentric heterochromatin involves a distinct pattern of histone modification and an RNA component. *Nature genetics* **30**, 329 (2002).

44. C. Muchardt, *et al.*, Coordinated methyl and RNA binding is required for heterochromatin localization of mammalian HP1α. *EMBO reports* **3**, 975–981 (2002).

45. R. R. Meehan, C.-F. Kao, S. Pennings, HP1 binding to native chromatin in vitro is determined by the hinge region and not by the chromodomain. *The EMBO journal* **22**, 3164–3174 (2003).

46. K. Hiragami-Hamada, *et al.*, Dynamic and flexible H3K9me3 bridging via HP1β dimerization establishes a plastic state of condensed chromatin. *Nature communications* **7**, 11310 (2016).

47. P. B. Singh, HP1 proteins—What is the essential interaction? *Russian Journal of Genetics* **46**, 1257–1262 (2010).

48. R. Aucott, *et al.*, HP1- is required for development of the cerebral neocortex and neuromuscular junctions. *The Journal of Cell Biology* **183**, 597–606 (2008).

49. R. S. Allan, *et al.*, An epigenetic silencing pathway controlling T helper 2 cell lineage commitment. *Nature* **487**, 249–253 (2012).

50. J. P. Brown, *et al.*, HP1γ function is required for male germ cell survival and spermatogenesis. *Epigenetics & Chromatin* **3**, 9 (2010).

51. K. Abe, *et al.*, Loss of heterochromatin protein 1 gamma reduces the number of primordial germ cells via impaired cell cycle progression in mice. *Biology of reproduction* **85**, 1013–1024 (2011).

52. Y. Takada, *et al.*, HP1γ links histone methylation marks to meiotic synapsis in mice. *Development* **138**, 4207–4217 (2011).

53. M. Lek, *et al.*, Analysis of protein-coding genetic variation in 60,706 humans. *Nature* **536**, 285 (2016).

54. M. Dundr, T. Misteli, Measuring dynamics of nuclear proteins by photobleaching. *Current protocols in cell biology* **18**, 13.5. 1-13.5. 18 (2003).

55. T. Cheutin, Maintenance of Stable Heterochromatin Domains by Dynamic HP1 Binding. *Science* **299**, 721–725 (2003).

56. R. Festenstein, *et al.*, Modulation of heterochromatin protein 1 dynamics in primary mammalian cells. *Science* **299**, 719–721 (2003).

57. L. Schmiedeberg, K. Weisshart, S. Diekmann, G. Meyer zu Hoerste, P. Hemmerich, High-and low-mobility populations of HP1 in heterochromatin of mammalian cells. *Molecular biology of the cell* **15**, 2819–2833 (2004).

58. G. K. Dialynas, Methylation-independent Binding to Histone H3 and Cell Cycle-dependent Incorporation of HP1beta into Heterochromatin. *Journal of Biological Chemistry* **281**, 14350–14360 (2006).

59. M. Billur, H. D. Bartunik, P. B. Singh, The essential function of HP1β: a case of the tail wagging the dog? *Trends in Biochemical Sciences* **35**, 115–123 (2010).

60. T. Misteli, Beyond the sequence: cellular organization of genome function. *Cell* **128**, 787–800 (2007).

61. C. D. Keating, Aqueous phase separation as a possible route to compartmentalization of biological molecules. *Accounts of chemical research* **45**, 2114–2124 (2012).

62. A. A. Hyman, C. A. Weber, F. Jülicher, Liquid-liquid phase separation in biology. *Annual review of cell and developmental biology* **30**, 39–58 (2014).

63. S. F. Banani, H. O. Lee, A. A. Hyman, M. K. Rosen, Biomolecular condensates: organizers of cellular biochemistry. *Nature reviews Molecular cell biology* **18**, 285 (2017).

64. X.-H. Li, P. L. Chavali, R. Pancsa, S. Chavali, M. M. Babu, Function and regulation of phase-separated biological condensates. *Biochemistry* **57**, 2452–2461 (2018).

65. J. Berry, S. C. Weber, N. Vaidya, M. Haataja, C. P. Brangwynne, RNA transcription modulates phase transition-driven nuclear body assembly. *Proceedings of the National Academy of Sciences* **112**, E5237–E5245 (2015).

66. H. Falahati, B. Pelham-Webb, S. Blythe, E. Wieschaus, Nucleation by rRNA dictates the precision of nucleolus assembly. *Current Biology* **26**, 277–285 (2016).

67. C. P. Brangwynne, T. J. Mitchison, A. A. Hyman, Active liquid-like behavior of nucleoli determines their size and shape in Xenopus laevis oocytes. *Proceedings of the National Academy of Sciences* **108**, 4334–4339 (2011).

68. M. Feric, *et al.*, Coexisting liquid phases underlie nucleolar subcompartments. *Cell* **165**, 1686–1697 (2016).

69. L. Wang, *et al.*, Histone Modifications Regulate Chromatin Compartmentalization by Contributing to a Phase Separation Mechanism. *Molecular Cell* (2019) https:/doi.org/10.1016/j.molcel.2019.08.019 (October 25, 2019).

70. Y. Shin, *et al.*, Liquid nuclear condensates mechanically sense and restructure the genome. *Cell* **175**, 1481-1491. e13 (2018).

71. F. Erdel, K. Rippe, Formation of chromatin subcompartments by phase separation. *Biophysical journal* **114**, 2262–2270 (2018).

72. C. C. Robinett, *et al.*, In vivo localization of DNA sequences and visualization of large-scale chromatin organization using lac operator/repressor recognition. *The Journal of cell biology* **135**, 1685–1700 (1996).

73. P. J. Wijchers, *et al.*, Characterization and dynamics of pericentromere-associated domains in mice. *Genome research* **25**, 958–969 (2015).

74. A. M. Azzaz, *et al.*, Human Heterochromatin Protein 1α Promotes Nucleosome Associations That Drive Chromatin Condensation. *Journal of Biological Chemistry* **289**, 6850–6861 (2014).

75. M. Hochstrasser, D. Mathog, Y. Gruenbaum, H. Saumweber, J. W. Sedat, Spatial organization of chromosomes in the salivary gland nuclei of Drosophila melanogaster. *The Journal of cell biology* **102**, 112–123 (1986).

76. K. P. Eagen, T. A. Hartl, R. D. Kornberg, Stable chromosome condensation revealed by chromosome conformation capture. *Cell* **163**, 934–946 (2015).

77. S. Machida, *et al.*, Structural Basis of Heterochromatin Formation by Human HP1. *Molecular Cell* **69**, 385-397.e8 (2018).

78. J. Mateos-Langerak, *et al.*, Spatially confined folding of chromatin in the interphase nucleus. *Proceedings of the National Academy of Sciences* **106**, 3812–3817 (2009).

79. C. Münkel, J. Langowski, Chromosome structure predicted by a polymer model. *Physical Review E* **57**, 5888 (1998).

80. P.-G. De Gennes, *Scaling concepts in polymer physics* (Cornell university press, 1979).

81. A. Y. Grosberg, A. R. Khokhlov, *Giant molecules: here, and there, and everywhere...* (1997).

82. R. Cortini, *et al.*, The physics of epigenetics. *Reviews of Modern Physics* **88**, 025002 (2016).

83. A. Lesage, V. Dahirel, J.-M. Victor, M. Barbi, Polymer coil–globule phase transition is a universal folding principle of Drosophila epigenetic domains. *Epigenetics & chromatin* **12**, 28 (2019).

84. L. A. Mirny, The fractal globule as a model of chromatin architecture in the cell. *Chromosome research* **19**, 37–51 (2011).

85. A. Pombo, M. Nicodemi, Physical mechanisms behind the large scale features of chromatin organization. *Transcription* **5**, e28447 (2014).

86. P. J. Flory, *Principles of polymer chemistry* (Cornell University Press, 1953).

87. K. Dušek, Phase separation in ternary systems induced by crosslinking. *Chemical Papers* **25**, 184–189 (1971).

88. J. F. Marko, Micromechanical studies of mitotic chromosomes. *Chromosome research* **16**, 469 (2008).

89. N. Saksouk, E. Simboeck, J. Déjardin, Constitutive heterochromatin formation and transcription in mammals. *Epigenetics & chromatin* **8**, 3 (2015).

90. B. McStay, Nucleolar organizer regions: genomic ‘dark matter’requiring illumination. *Genes & Development* **30**, 1598–1610 (2016).

91. R. C. Allshire, H. D. Madhani, Ten principles of heterochromatin formation and function. *Nature Reviews Molecular Cell Biology* **19**, 229 (2018).

92. A. Janssen, S. U. Colmenares, G. H. Karpen, Heterochromatin: guardian of the genome. *Annual review of cell and developmental biology* **34**, 265–288 (2018).

93. M. E. Blewitt, *et al.*, An N-ethyl-N-nitrosourea screen for genes involved in variegation in the mouse. *Proceedings of the National Academy of Sciences* **102**, 7629–7634 (2005).

94. B. D. Fodor, N. Shukeir, G. Reuter, T. Jenuwein, Mammalian Su (var) genes in chromatin control. *Annual review of cell and developmental biology* **26**, 471–501 (2010).

95. I. Solovei, K. Thanisch, Y. Feodorova, How to rule the nucleus: divide et impera. *Current opinion in cell biology* **40**, 47–59 (2016).

96. A. J. Ruthenburg, H. Li, D. J. Patel, C. D. Allis, Multivalent engagement of chromatin modifications by linked binding modules. *Nature reviews Molecular cell biology* **8**, 983 (2007).

97. Z. Wang, D. J. Patel, Combinatorial readout of dual histone modifications by paired chromatin-associated modules. *Journal of Biological Chemistry* **286**, 18363–18368 (2011).

98. P. B. Singh, *et al.*, A sequence motif found in a Drosophila heterochromatin protein is conserved in animals and plants. *Nucleic acids research* **19**, 789–794 (1991).

99. P. B. Singh, Molecular mechanisms of cellular determination: their relation to chromatin structure and parental imprinting. *Journal of cell science* **107**, 2653–2668 (1994).

100. P. B. Singh, Heterochromatin and the molecular mechanisms of 'parent-of-origin' effects in animals. *Journal of Biosciences* **41**, 759–786 (2016).

101. P. Mombaerts, The human repertoire of odorant receptor genes and pseudogenes. *Annual review of genomics and human genetics* **2**, 493–510 (2001).

102. X. Zhang, X. Zhang, S. Firestein, Comparative genomics of odorant and pheromone receptor genes in rodents. *Genomics* **89**, 441–450 (2007).

103. S. Lomvardas, T. Maniatis, Histone and DNA modifications as regulators of neuronal development and function. *Cold Spring Harbor perspectives in biology* **8**, a024208 (2016).

104. M. J. Vogel, *et al.*, Human heterochromatin proteins form large domains containing KRAB-ZNF genes. *Genome Research* **16**, 1493–1504 (2006).

105. S. S. P. Rao, *et al.*, A 3D Map of the Human Genome at Kilobase Resolution Reveals Principles of Chromatin Looping. *Cell* **159**, 1665–1680 (2014).

106. Y. Jiang, *et al.*, The methyltransferase SETDB1 regulates a large neuron-specific topological chromatin domain. *Nature Genetics* **49**, 1239–1250 (2017).

107. S. Matoba, *et al.*, Embryonic Development following Somatic Cell Nuclear Transfer Impeded by Persisting Histone Methylation. *Cell* **159**, 884–895 (2014).

108. M. S. H. Ko, “Zygotic genome activation revisited: looking through the expression and function of Zscan4” in *Current Topics in Developmental Biology*, (Elsevier, 2016), pp. 103–124.

109. J. S. Becker, *et al.*, Genomic and proteomic resolution of heterochromatin and its restriction of alternate fate genes. *Molecular cell* **68**, 1023-1037. e15 (2017).

110. D. Nicetto, *et al.*, H3K9me3-heterochromatin loss at protein-coding genes enables developmental lineage specification. *Science* **363**, 294–297 (2019).

111. S. Cheloufi, *et al.*, The histone chaperone CAF-1 safeguards somatic cell identity. *Nature* **528**, 218 (2015).

112. M. Borkent, *et al.*, A serial shRNA screen for roadblocks to reprogramming identifies the protein modifier SUMO2. *Stem cell reports* **6**, 704–716 (2016).

113. A. C. Groner, *et al.*, KRAB–zinc finger proteins and KAP1 can mediate long-range transcriptional repression through heterochromatin spreading. *PLoS genetics* **6**, e1000869 (2010).

114. K. Regha, *et al.*, Active and repressive chromatin are interspersed without spreading in an imprinted gene cluster in the mammalian genome. *Molecular cell* **27**, 353–366 (2007).

115. S. Bilodeau, M. H. Kagey, G. M. Frampton, P. B. Rahl, R. A. Young, SetDB1 contributes to repression of genes encoding developmental regulators and maintenance of ES cell state. *Genes & development* **23**, 2484–2489 (2009).

116. Roadmap Epigenomics Consortium, *et al.*, Integrative analysis of 111 reference human epigenomes. *Nature* **518**, 317 (2015).

117. J. Molitor, J.-P. Mallm, K. Rippe, F. Erdel, Retrieving chromatin patterns from deep sequencing data using correlation functions. *Biophysical journal* **112**, 473–490 (2017).

118. G. Ecco, M. Imbeault, D. Trono, KRAB zinc finger proteins. *Development* **144**, 2719–2729 (2017).

119. S. Iyengar, P. J. Farnham, KAP1 Protein: An Enigmatic Master Regulator of the Genome. *Journal of Biological Chemistry* **286**, 26267–26276 (2011).

120. H. O’Geen, *et al.*, Genome-wide analysis of KAP1 binding suggests autoregulation of KRAB-ZNFs. *PLoS genetics* **3**, e89 (2007).

121. S. Frietze, H. O’Geen, K. R. Blahnik, V. X. Jin, P. J. Farnham, ZNF274 recruits the histone methyltransferase SETDB1 to the 3′ ends of ZNF genes. *PloS one* **5**, e15082 (2010).

122. J. R. Friedman, *et al.*, KAP-1, a novel corepressor for the highly conserved KRAB repression domain. *Genes & development* **10**, 2067–2078 (1996).

123. B. Le Douarin, *et al.*, A possible involvement of TIF1 alpha and TIF1 beta in the epigenetic control of transcription by nuclear receptors. *The EMBO journal* **15**, 6701–6715 (1996).

124. P. Moosmann, O. Georgiev, B. Le Douarin, J.-P. Bourquin, W. Schaffner, Transcriptional repression by RING finger protein TIF1β that interacts with the KRAB repressor domain of KOX1. *Nucleic acids research* **24**, 4859–4867 (1996).

125. A. V. Ivanov, *et al.*, PHD Domain-Mediated E3 Ligase Activity Directs Intramolecular Sumoylation of an Adjacent Bromodomain Required for Gene Silencing. *Molecular Cell* **28**, 823–837 (2007).

126. B. X. Yang, *et al.*, Systematic Identification of Factors for Provirus Silencing in Embryonic Stem Cells. *Cell* **163**, 230–245 (2015).

127. R. F. Ryan, *et al.*, KAP-1 corepressor protein interacts and colocalizes with heterochromatic and euchromatic HP1 proteins: a potential role for Krüppel-associated box–zinc finger proteins in heterochromatin-mediated gene silencing. *Molecular and cellular biology* **19**, 4366–4378 (1999).

128. M. S. Lechner, G. E. Begg, D. W. Speicher, F. J. Rauscher, Molecular determinants for targeting heterochromatin protein 1-mediated gene silencing: direct chromoshadow domain–KAP-1 corepressor interaction is essential. *Molecular and Cellular Biology* **20**, 6449–6465 (2000).

129. S. J. Elsässer, K.-M. Noh, N. Diaz, C. D. Allis, L. A. Banaszynski, Histone H3.3 is required for endogenous retroviral element silencing in embryonic stem cells. *Nature* **522**, 240–244 (2015).

130. P. Drané, K. Ouararhni, A. Depaux, M. Shuaib, A. Hamiche, The death-associated protein DAXX is a novel histone chaperone involved in the replication-independent deposition of H3. 3. *Genes & development* **24**, 1253–1265 (2010).

131. A. D. Goldberg, *et al.*, Distinct factors control histone variant H3. 3 localization at specific genomic regions. *Cell* **140**, 678–691 (2010).

132. L. H. Wong, *et al.*, ATRX interacts with H3. 3 in maintaining telomere structural integrity in pluripotent embryonic stem cells. *Genome research* **20**, 351–360 (2010).

133. D. Valle-Garcia, *et al.*, ATRX binds to atypical chromatin domains at the 3′ exons of zinc finger genes to preserve H3K9me3 enrichment. *Epigenetics* **11**, 398–414 (2016).

134. S. Eustermann, *et al.*, Combinatorial readout of histone H3 modifications specifies localization of ATRX to heterochromatin. *Nat Struct Mol Biol* **18**, 777–782 (2011).

135. N. Kourmouli, Y. Sun, S. van der Sar, P. B. Singh, J. P. Brown, Epigenetic regulation of mammalian pericentric heterochromatin in vivo by HP1. *Biochemical and Biophysical Research Communications* **337**, 901–907 (2005).

136. D. C. Schultz, J. R. Friedman, F. J. Rauscher, Targeting histone deacetylase complexes via KRAB-zinc finger proteins: the PHD and bromodomains of KAP-1 form a cooperative unit that

recruits a novel isoform of the Mi-2α subunit of NuRD. *Genes & development* **15**, 428–443 (2001).

137. D. C. Schultz, K. Ayyanathan, D. Negorev, G. G. Maul, F. J. Rauscher, SETDB1: a novel KAP-1-associated histone H3, lysine 9-specific methyltransferase that contributes to HP1-mediated silencing of euchromatic genes by KRAB zinc-finger proteins. *Genes & development* **16**, 919–932 (2002).

138. K. Ayyanathan, Regulated recruitment of HP1 to a euchromatic gene induces mitotically heritable, epigenetic gene silencing: a mammalian cell culture model of gene variegation. *Genes & Development* **17**, 1855–1869 (2003).

139. S. P. Sripathy, J. Stevens, D. C. Schultz, The KAP1 corepressor functions to coordinate the assembly of de novo HP1-demarcated microenvironments of heterochromatin required for KRAB zinc finger protein-mediated transcriptional repression. *Molecular and cellular biology* **26**, 8623–8638 (2006).

140. P. B. Singh, V. V. Shloma, S. N. Belyakin, Maternal regulation of chromosomal imprinting in animals. *Chromosoma*, 1–12 (2019).

141. M. Wiznerowicz, *et al.*, The Krüppel-associated box repressor domain can trigger de novo promoter methylation during mouse early embryogenesis. *Journal of Biological Chemistry* **282**, 34535–34541 (2007).

142. H. M. Rowe, *et al.*, De novo DNA methylation of endogenous retroviruses is shaped by KRAB-ZFPs/KAP1 and ESET. *Development* **140**, 519–529 (2013).

143. S. Quenneville, *et al.*, In embryonic stem cells, ZFP57/KAP1 recognize a methylated hexanucleotide to affect chromatin and DNA methylation of imprinting control regions. *Molecular cell* **44**, 361–372 (2011).

144. X. Zuo, *et al.*, The zinc finger protein ZFP57 requires its cofactor to recruit DNA methyltransferases and maintains the DNA methylation imprint in embryonic stem cells via its transcriptional repression domain. *Journal of Biological Chemistry*, jbc. M111. 322644 (2011).

145. F. Fuks, P. J. Hurd, R. Deplus, T. Kouzarides, The DNA methyltransferases associate with HP1 and the SUV39H1 histone methyltransferase. *Nucl. Acids Res.* **31**, 2305–2312 (2003).

146. A. Smallwood, P.-O. Esteve, S. Pradhan, M. Carey, Functional cooperation between HP1 and DNMT1 mediates gene silencing. *Genes & Development* **21**, 1169–1178 (2007).

147. M. M. Müller, B. Fierz, L. Bittova, G. Liszczak, T. W. Muir, A two-state activation mechanism controls the histone methyltransferase Suv39h1. *Nature chemical biology* **12**, 188 (2016).

148. M. Melcher, *et al.*, Structure-function analysis of SUV39H1 reveals a dominant role in heterochromatin organization, chromosome segregation, and mitotic progression. *Molecular and cellular biology* **20**, 3728–3741 (2000).

149. I. M. Krouwels, *et al.*, A glue for heterochromatin maintenance: stable SUV39H1 binding to heterochromatin is reinforced by the SET domain. *The Journal of cell biology* **170**, 537–549 (2005).

150. N. A. Hathaway, *et al.*, Dynamics and Memory of Heterochromatin in Living Cells. *Cell* **149**, 1447–1460 (2012).

151. D. Chetverina, *et al.*, Boundaries of loop domains (insulators): Determinants of chromosome form and function in multicellular eukaryotes. *Bioessays* **39**, 1600233 (2017).

152. J. Wang, S. T. Lawry, A. L. Cohen, S. Jia, Chromosome boundary elements and regulation of heterochromatin spreading. *Cellular and Molecular Life Sciences* **71**, 4841–4852 (2014).

153. W. Fischle, *et al.*, Regulation of HP1–chromatin binding by histone H3 methylation and phosphorylation. *Nature* **438**, 1116 (2005).

154. D. Michieletto, *et al.*, Shaping epigenetic memory via genomic bookmarking. *Nucleic acids research* **46**, 83–93 (2017).

155. J. E. Mermoud, S. P. Rowbotham, P. D. Varga-Weisz, Keeping chromatin quiet: how nucleosome remodeling restores heterochromatin after replication. *Cell cycle* **10**, 4017–4025 (2011).

156. S. P. Rowbotham, *et al.*, Maintenance of silent chromatin through replication requires SWI/SNF-like chromatin remodeler SMARCAD1. *Molecular cell* **42**, 285–296 (2011).

157. A. Loyola, *et al.*, The HP1α–CAF1–SetDB1-containing complex provides H3K9me1 for Suv39-mediated K9me3 in pericentric heterochromatin. *EMBO reports* **10**, 769–775 (2009).

158. N. Murzina, A. Verreault, E. Laue, B. Stillman, Heterochromatin dynamics in mouse cells: interaction between chromatin assembly factor 1 and HP1 proteins. *Molecular cell* **4**, 529–540 (1999).

159. E. E. Eichler, *et al.*, Complex β-satellite repeat structures and the expansion of the zinc finger gene cluster in 19p12. *Genome research* **8**, 791–808 (1998).

160. L. M. Armelin-Correa, L. M. Gutiyama, D. Y. Brandt, B. Malnic, Nuclear compartmentalization of odorant receptor genes. *Proceedings of the National Academy of Sciences* **111**, 2782–2787 (2014).

161. F. S. Bates, Polymer-polymer phase behavior. *Science* **251**, 898–905 (1991).

162. I. W. Hamley, *The physics of block copolymers* (Oxford University Press Oxford, 1998).

163. Q. MacPherson, B. Beltran, A. J. Spakowitz, Bottom–up modeling of chromatin segregation due to epigenetic modifications. *Proceedings of the National Academy of Sciences* **115**, 12739–12744 (2018).

164. J. Nuebler, G. Fudenberg, M. Imakaev, N. Abdennur, L. A. Mirny, Chromatin organization by an interplay of loop extrusion and compartmental segregation. *Proceedings of the National Academy of Sciences* **115**, E6697–E6706 (2018).

165. M. Di Pierro, D. A. Potoyan, P. G. Wolynes, J. N. Onuchic, Anomalous diffusion, spatial coherence, and viscoelasticity from the energy landscape of human chromosomes. *Proceedings of the National Academy of Sciences* **115**, 7753–7758 (2018).

166. L. A. Mirny, M. Imakaev, N. Abdennur, Two major mechanisms of chromosome organization. *Current opinion in cell biology* **58**, 142–152 (2019).

167. J. Dekker, M. A. Marti-Renom, L. A. Mirny, Exploring the three-dimensional organization of genomes: interpreting chromatin interaction data. *Nature Reviews Genetics* **14**, 390 (2013).

168. J. R. Dixon, *et al.*, Chromatin architecture reorganization during stem cell differentiation. *Nature* **518**, 331–336 (2015).

169. B. Bonev, G. Cavalli, Organization and function of the 3D genome. *Nature Reviews Genetics* **17**, 661 (2016).

170. Q. Szabo, F. Bantignies, G. Cavalli, Principles of genome folding into topologically associating domains. *Science advances* **5**, eaaw1668 (2019).

171. W. Schwarzer, *et al.*, Two independent modes of chromatin organization revealed by cohesin removal. *Nature* **551**, 51 (2017).

172. L. Vian, *et al.*, The Energetics and Physiological Impact of Cohesin Extrusion. *Cell* **173**, 1165-1178.e20 (2018).

173. F. S. Bates, G. H. Fredrickson, Block copolymer thermodynamics: theory and experiment. *Annual review of physical chemistry* **41**, 525–557 (1990).

174. H. Belaghzal, *et al.*, Compartment-dependent chromatin interaction dynamics revealed by liquid chromatin Hi-C. *bioRxiv*, 704957 (2019).

175. N. Saksouk, *et al.*, The mouse HP1 proteins are essential for preventing liver tumorigenesis. *bioRxiv*, 441279 (2019).

176. B. Van Steensel, A. S. Belmont, Lamina-associated domains: links with chromosome architecture, heterochromatin, and gene repression. *Cell* **169**, 780–791 (2017).

177. I. Solovei, *et al.*, LBR and lamin A/C sequentially tether peripheral heterochromatin and inversely regulate differentiation. *Cell* **152**, 584–598 (2013).

178. M. Falk, *et al.*, Heterochromatin drives compartmentalization of inverted and conventional nuclei. *Nature* **570**, 395–399 (2019).

179. I. Solovei, *et al.*, Nuclear architecture of rod photoreceptor cells adapts to vision in mammalian evolution. *Cell* **137**, 356–368 (2009).

180. Y. Mai, A. Eisenberg, Self-assembly of block copolymers. *Chemical Society Reviews* **41**, 5969–5985 (2012).

181. D. E. Discher, A. Eisenberg, Polymer vesicles. *Science* **297**, 967–973 (2002).

182. P. B. Singh, N. S. Huskisson, Chromatin complexes as aperiodic microcrystalline arrays that regulate genome organisation and expression. *Developmental genetics* **22**, 85–99 (1998).

183. K. S. Weiler, B. T. Wakimoto, Heterochromatin and gene expression in Drosophila. *Annual review of genetics* **29**, 577–605 (1995).

184. R. H. Devlin, B. Bingham, B. T. Wakimoto, The organization and expression of the light gene, a heterochromatic gene of Drosophila melanogaster. *Genetics* **125**, 129–140 (1990).

185. B. T. Wakimoto, M. G. Hearn, The effects of chromosome rearrangements on the expression of heterochromatic genes in chromosome 2L of Drosophila melanogaster. *Genetics* **125**, 141–154 (1990).

186. S. Henikoff, J. M. Jackson, P. B. Talbert, Distance and pairing effects on the brownDominant heterochromatic element in Drosophila. *Genetics* **140**, 1007–1017 (1995).

187. K. Sander, The evolution of patterning mechanisms: gleanings from insect embryogenesis. *Development and evolution*, 137–59 (1983).

188. L. Wolpert, *The Triumph of the Embryo* (Oxford University Press, 1991).

189. J. M. Slack, P. W. Holland, C. F. Graham, The zootype and the phylotypic stage. *Nature* **361**, 490–492 (1993).

190. N. Irie, S. Kuratani, The developmental hourglass model: a predictor of the basic body plan? *Development* **141**, 4649–4655 (2014).

191. D. Duboule, Temporal colinearity and the phylotypic progression: a basis for the stability of a vertebrate Bauplan and the evolution of morphologies through heterochrony. *Development* **1994**, 135–142 (1994).

192. R. A. Raff, Developmental mechanisms in the evolution of animal form: origins and evolvability of body plans. *Early life on earth* **84**, 489–500 (1994).

193. D. Nicetto, K. S. Zaret, Role of H3K9me3 heterochromatin in cell identity establishment and maintenance. *Current opinion in genetics & development* **55**, 1–10 (2019).

194. S. L. Peek, K. M. Mah, J. A. Weiner, Regulation of neural circuit formation by protocadherins. *Cellular and molecular life sciences* **74**, 4133–4157 (2017).

195. S. J. Gaunt, P. B. Singh, Homeogene expression patterns and chromosomal imprinting. *Trends in genetics: TIG* **6**, 208–212 (1990).

196. R. Paro, Imprinting a determined state into the chromatin of Drosophila. *Trends in Genetics* **6**, 416–421 (1990).

197. A. J. Plys, *et al.*, Phase separation of Polycomb-repressive complex 1 is governed by a charged disordered region of CBX2. *Genes & development* (2019).

198. R. Tatavosian, *et al.*, Nuclear condensates of the Polycomb protein chromobox 2 (CBX2) assemble through phase separation. *Journal of Biological Chemistry* **294**, 1451–1463 (2019).

199. D. Reinberg, L. D. Vales, Chromatin domains rich in inheritance. *Science* **361**, 33–34 (2018).

200. A. Mattout, *et al.*, Heterochromatin Protein 1β (HP1β) has distinct functions and distinct nuclear distribution in pluripotent versus differentiated cells. *Genome Biology* **16** (2015).

201. B. Langmead, S. L. Salzberg, Fast gapped-read alignment with Bowtie 2. *Nature methods* **9**, 357 (2012).

202. F. Ramírez, *et al.*, deepTools2: a next generation web server for deep-sequencing data analysis. *Nucleic Acids Research* **44**, W160–W165 (2016).

203. J. Köster, S. Rahmann, Snakemake—a scalable bioinformatics workflow engine. *Bioinformatics* **28**, 2520–2522 (2012).

204. Y. Wang, *et al.*, The 3D Genome Browser: a web-based browser for visualizing 3D genome organization and long-range chromatin interactions. *Genome Biology* **19**, 151 (2018).

205. G. A. Stoll, *et al.*, Structure of KAP1 tripartite motif identifies molecular interfaces required for retroelement silencing. *PNAS* **116**, 15042–15051 (2019).

206. International Human Genome Sequencing Consortium, Finishing the euchromatic sequence of the human genome. *Nature* **431**, 931–945 (2004).

207. A. Eymery, M. Callanan, C. Vourc'h, The secret message of heterochromatin: new insights into the mechanisms and function of centromeric and pericentric repeat sequence transcription. *International Journal of Developmental Biology* **53**, 259–268 (2009).

208. A. H. F. M. Peters, *et al.*, Loss of the Suv39h Histone Methyltransferases Impairs Mammalian Heterochromatin and Genome Stability. *Cell* **107**, 323–337 (2001).

209. B. Lehnertz, *et al.*, Suv39h-mediated histone H3 lysine 9 methylation directs DNA methylation to major satellite repeats at pericentric heterochromatin. *Current Biology* **13**, 1192–1200 (2003).

210. I. G. Cowell, *et al.*, Heterochromatin, HP1 and methylation at lysine 9 of histone H3 in animals. *Chromosoma* **111**, 22–36 (2002).

211. G. Schotta, A silencing pathway to induce H3-K9 and H4-K20 trimethylation at constitutive heterochromatin. *Genes & Development* **18**, 1251–1262 (2004).

212. W. S. Saunders, *et al.*, Molecular cloning of a human homologue of Drosophila heterochromatin protein HP1 using anti-centromere autoantibodies with anti-chromo specificity. *Journal of Cell Science* **104**, 573–582 (1993).

213. K. A. Wreggett, *et al.*, A mammalian homologue of Drosophila heterochromatin protein 1 (HP1) is a component of constitutive heterochromatin. *Cytogenetic and Genome Research* **66**, 99–103 (1994).

214. D. Horsley, A. Hutchings, G. W. Butcher, P. B. Singh, M32, a murine homologue of Drosophila heterochromatin protein 1 (HP1), localises to euchromatin within interphase nuclei and is largely excluded from constitutive heterochromatin. *Cytogenetic and Genome Research* **73**, 308–311 (1996).

215. H. Leonhardt, A. W. Page, H.-U. Weier, T. H. Bestor, A targeting sequence directs DNA methyltransferase to sites of DNA replication in mammalian nuclei. *Cell* **71**, 865–873 (1992).

216. R. Z. Jurkowska, *et al.*, Oligomerization and binding of the Dnmt3a DNA methyltransferase to parallel DNA molecules heterochromatic localization and role of Dnmt3L. *Journal of Biological Chemistry* **286**, 24200–24207 (2011).

217. K. E. Bachman, M. R. Rountree, S. B. Baylin, Dnmt3a and Dnmt3b Are Transcriptional Repressors That Exhibit Unique Localization Properties to Heterochromatin. *Journal of Biological Chemistry* **276**, 32282–32287 (2001).

218. B. W. Lubit, P. T. Duc, O. J. Miller, B. F. Erlanger, Localization of 5-methylcytosine in human metaphase chromosomes by immunoelectron microscopy. *Cell* **9**, 503–509 (1976).

219. C. Baumann, A. Schmidtmann, K. Muegge, R. De La Fuente, Association of ATRX with pericentric heterochromatin and the Y chromosome of neonatal mouse spermatogonia. *BMC molecular biology* **9**, 29 (2008).

220. R. Papait, *et al.*, The PHD domain of Np95 (mUHRF1) is involved in large-scale reorganization of pericentromeric heterochromatin. *Molecular biology of the cell* **19**, 3554–3563 (2008).

221. Y. Liu, H. Toh, H. Sasaki, X. Zhang, X. Cheng, An atomic model of Zfp57 recognition of CpG methylation within a specific DNA sequence. *Genes & development* **26**, 2374–2379 (2012).

222. E. V. Chambers, W. A. Bickmore, C. A. Semple, Divergence of mammalian higher order chromatin structure is associated with developmental loci. *PLoS computational biology* **9**, e1003017 (2013).

223. M. García-Cao, R. O'Sullivan, A. H. Peters, T. Jenuwein, M. A. Blasco, Epigenetic regulation of telomere length in mammalian cells by the Suv39h1 and Suv39h2 histone methyltransferases. *Nature genetics* **36**, 94 (2004).

224. M. A. Blasco, The epigenetic regulation of mammalian telomeres. *Nature Reviews Genetics* **8**, 299–309 (2007).

225. S. Gonzalo, *et al.*, Role of the RB1 family in stabilizing histone methylation at constitutive heterochromatin. *Nature cell biology* **7**, 420 (2005).

226. R. Benetti, M. García-Cao, M. A. Blasco, Telomere length regulates the epigenetic status of mammalian telomeres and subtelomeres. *Nature genetics* **39**, 243 (2007).

227. K.-M. Schmitz, C. Mayer, A. Postepska, I. Grummt, Interaction of noncoding RNA with the rDNA promoter mediates recruitment of DNMT3b and silencing of rRNA genes. *Genes & development* **24**, 2264–2269 (2010).

228. D. M. Stults, M. W. Killen, H. H. Pierce, A. J. Pierce, Genomic architecture and inheritance of human ribosomal RNA gene clusters. *Genome research* **18**, 13–18 (2008).

229. A. Murayama, *et al.*, Epigenetic control of rDNA loci in response to intracellular energy status. *Cell* **133**, 627–639 (2008).

230. R. Chakrabarti, *et al.*, Phosphatidylinositol-4-phosphate 5-Kinase 1α Modulates Ribosomal RNA Gene Silencing through Its Interaction with Histone H3 Lysine 9 Trimethylation and Heterochromatin Protein HP1-α. *Journal of Biological Chemistry* **290**, 20893–20903 (2015).

231. C. Guetg, *et al.*, The NoRC complex mediates the heterochromatin formation and stability of silent rRNA genes and centromeric repeats. *The EMBO journal* **29**, 2135–2146 (2010).

232. H. Bierhoff, *et al.*, Quiescence-Induced LncRNAs Trigger H4K20 Trimethylation and Transcriptional Silencing. *Molecular Cell* **54**, 675–682 (2014).

233. R. Santoro, J. Li, I. Grummt, The nucleolar remodeling complex NoRC mediates heterochromatin formation and silencing of ribosomal gene transcription. *Nature Genetics* **32**, 393–396 (2002).

234. T. Gagnon-Kugler, F. Langlois, V. Stefanovsky, F. Lessard, T. Moss, Loss of human ribosomal gene CpG methylation enhances cryptic RNA polymerase II transcription and disrupts ribosomal RNA processing. *Molecular cell* **35**, 414–425 (2009).

235. L. M. Rapkin, *et al.*, The histone chaperone DAXX maintains the structural organization of heterochromatin domains. *Epigenetics & chromatin* **8**, 44 (2015).

236. T. D. Matheson, P. D. Kaufman, Grabbing the genome by the NADs. *Chromosoma* **125**, 361–371 (2016).

237. A. Magklara, *et al.*, An epigenetic signature for monoallelic olfactory receptor expression. *Cell* **145**, 555–570 (2011).

238. D. B. Lyons, *et al.*, Heterochromatin-mediated gene silencing facilitates the diversification of olfactory neurons. *Cell reports* **9**, 884–892 (2014).

239. E. J. Clowney, *et al.*, Nuclear aggregation of olfactory receptor genes governs their monogenic expression. *Cell* **151**, 724–737 (2012).

240. J. Chen, *et al.*, H3K9 methylation is a barrier during somatic cell reprogramming into iPSCs. *Nature genetics* **45**, 34 (2013).

241. R. Sridharan, *et al.*, Proteomic and genomic approaches reveal critical functions of H3K9 methylation and heterochromatin protein-1γ in reprogramming to pluripotency. *Nat. Cell Biol.* **15**, 872–882 (2013).

242. D. Leung, *et al.*, Regulation of DNA methylation turnover at LTR retrotransposons and imprinted loci by the histone methyltransferase Setdb1. *PNAS* **111**, 6690–6695 (2014).

243. R. Strogantsev, *et al.*, Allele-specific binding of ZFP57 in the epigenetic regulation of imprinted and non-imprinted monoallelic expression. *Genome biology* **16**, 112 (2015).

244. M. Pannetier, *et al.*, PR-SET7 and SUV4-20H regulate H4 lysine-20 methylation at imprinting control regions in the mouse. *EMBO reports* **9**, 998–1005 (2008).

245. E. Li, C. Beard, R. Jaenisch, Role for DNA methylation in genomic imprinting. *Nature* **366**, 362 (1993).

246. H. Kobayashi, *et al.*, Contribution of intragenic DNA methylation in mouse gametic DNA methylomes to establish oocyte-specific heritable marks. *PLoS genetics* **8**, e1002440 (2012).

247. H. P. Voon, *et al.*, ATRX plays a key role in maintaining silencing at interstitial heterochromatic loci and imprinted genes. *Cell reports* **11**, 405–418 (2015).

248. D. M. Messerschmidt, B. B. Knowles, D. Solter, DNA methylation dynamics during epigenetic reprogramming in the germline and preimplantation embryos. *Genes & development* **28**, 812–828 (2014).

Constitutive Heterochromatins	**Size**	**H3K9MTases**	**H3K9me3**	**H4K20MTase**	**H4K20me3**	**HP1**	**DNMTases**	**5mC**	**Np95**	**ATRX/ DAXX**	**H3.3**	**KAP1**	**Compartment/ TAD**
Peri-centric	**Human** ~ 0.2 – 20Mb [(206)] **Mouse** ~6Mb [(207)]	✓ SUV39H1/2 [(208, 209)] G9a/GLP [(156)] SETDB1 [(157)]	✓ [(210)]	✓ SuvH4201/2 [(211)]	✓ [(30, 211)]	✓ HP1α [(30, 212)] HP1β [(30, 213)] HP1γ [(30, 214)]	✓ DNMT1 [(215)] DNMT3A [(216)] DNMT3B [(217)]	✓ [(218, 219)]	✓ [(220, 221)]	✓ [c]	✓ [(130–132)]	✓ [(157)]	**PAD** **Identified by 4C not Hi-C** [(73)]
Telomeric plus sub-telomeric	**Human** ~10-300Kb [(206)] **Mouse** ~5Mb [(222)]	✓ SUV39H1/2 [(223)]	✓ [(223, 224)]	✓ SuvH4201/2 [(224, 225)]	✓ [(224–226)]	✓ HP1α HP1β [(224–226)]	✓ DNMT1 DNMT3A DNMT3B [(224–226)]	✓ [(224–226)]	**NK**	✓ [(224–226)]	✓ [(224–226)]	**NK**	**TPE-OLD** [(227)]
NOR plus peri-nucleolar	**Human** ~0.25 to 6.5Mb [(90, 228)] **Mouse** **NK**	✓ SUV39H1 [(229)]	✓ [(230, 231)]	✓ SuvH420/2 [(232)]	✓ [(231)]	✓ HP1α HP1β HP1γ [(233)]	✓ DNMT1 DNMT3A [(227, 233, 234)]	✓ [(233, 234)]	**NK**	✓ [(235)]	✓ [(235)]	**NK**	**NAD** [(236)]
Heterochromatin-like *domains*	**Size**	**H3K9MTases**	**H3K9me3**	**H4K20MTase**	**H4K20me3**	**HP1**	**DNMTases**	**5mC**	**Np95**	**ATRX/ DAXX**	**H3.3**	**KAP1**	**Compartment/ TAD**
Odorant receptors	**Human** 0.1 to 1Mb [(101)] **Mouse** 1 to 5 Mb [(102)]	✓ G9a/GLP [(237)]	✓ [(237, 238)]	✓ SuvH4201/2 [(237)]	✓ [(237, 238)]	✓ HP1β [(239)]	**NK**	**NK**	**NK**	**NK**	**NK**	**NK**	**Predominantly B2** **[This study]**
KRAB-ZNF gene clusters	**Human and mouse** Up to 4Mb [(104)]	✓ SUV39H1 [(104)]	✓ [(104, 113)]	**NK**	**NK**	✓ HP1β [(104, 113)]	**NK**	**NK**	**NK**	**NK**	**NK**	✓ [(113)]	**B4 sub-compartment** [(105)]
SCNT Reprogramming Resistant Regions (RRRs)	**Human** **NK** **Mouse** Up to 2Mb [(50)]	✓ SUV39H1 [(50)]	✓ [(50)]	**NK**	**NK**	**NK**	**NK**	**NK**	**NK**	**NK**	**NK**	**NK**	**Mixed A and B** **[This study]**
Procadherin cluster superTAD	**Human and mouse** 1.2MB [(51)]	✓ SETDB1 [(51)]	✓ [(51)]	**NK**	**NK**	**NK**	**NK**	**NK**	**NK**	**NK**	**NK**	**NK**	**superTAD** [(51)] **B3 sub-compartment** **[This study]**
Sonication resistant heterochromatin (srHC)	**Human** Average size 0.135MB [(107)]	**NK**	✓ [(107, 110)]	**NK**	**NK**	**NK**	**NK**	**NK**	**NK**	**NK**	**NK**	**NK**	**Predominantly B2** **[This study]**

Heterochromatin-like *complexes*	**Size**	**H3K9MTases**	**H3K9me3**	**H4K20MTase**	**H4K20me3**	**HP1**	**DNMTases**	**5mC**	**Np95**	**ATRX/ DAXX**	**H3.3**	**KAP1**	**Compartment/ TAD**
3' end of KRAB-ZNF genes	**Human and mouse** ~6Kb [(104)]	✓ SETDB1 [(119, 121)]	✓ [(119, 133)]	**NK**	**NK**	✓ HP1β [(104, 113)]	**NK**	**NK**	**NK**	✓ [(119)]	✓ [(119)]	✓ [(119, 120, 137)]	**B4 sub-compartment** [(105)]
IPS reprogramming resistant regions	**Human NK** **Mouse NK**	✓ SETDB1 [(115, 240)]	✓ [(115, 240, 241)]	**NK**	**NK**	✓ HP1γ [(241)]	**NK**	**NK**	**NK**	**NK**	**NK**	**NK**	**NK**
Imprinted gDMRs	**Human NK Mouse** ~6Kb [(114)]	✓ SETDB1 [(242)]	✓ [(114, 242, 243)]	✓ SuvH4201/2 [(244)]	✓ [(114, 243, 244)]	✓ HP1α HP1β [(114)] HP1γ [(114, 143, 243)]	✓ DNMT1 DNMT3A DNMT3B [(143, 144)]	✓ [(146, 245, 246)]	✓ [(143)]	✓ [(247)]	✓ [(247)]	✓ [(143, 248)]	**Mixed: A and B [This study]**

Table 1: Major structural and enzymatic constituents, along with histone/DNA modifications, associated with mammalian constitutive heterochromatin, which are shared with heterochromatin-like domains/complexes. ✓ = present. **NK** = not known. References are in square brackets and are to be found in the reference list.

Taken and modified from (100).

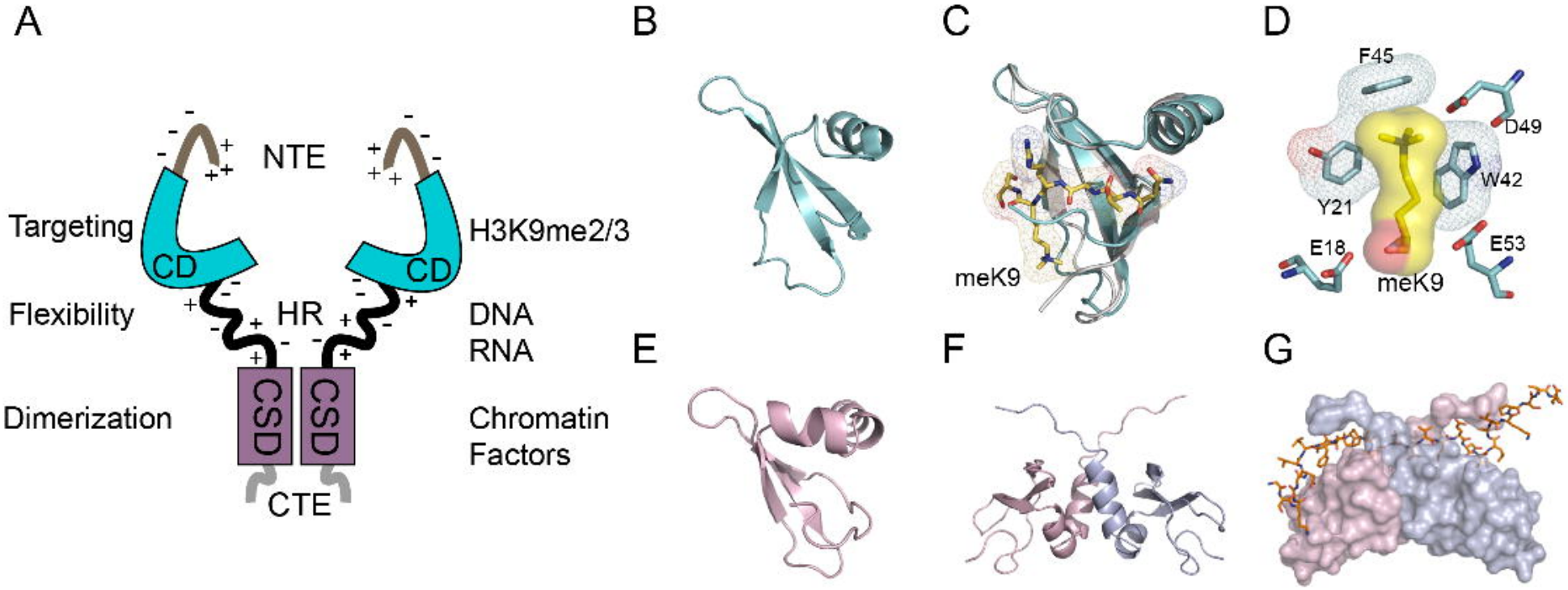
A
NTE
Targeting
CD
CD
H3K9me2/3
Flexibility
HR
DNA
RNA
Dimerization
CSD
CSD
Chromatin
Factors
CTE
B
C
meK9
D
F45
D49
W42
Y21
E18
E53
meK9
E
F
G

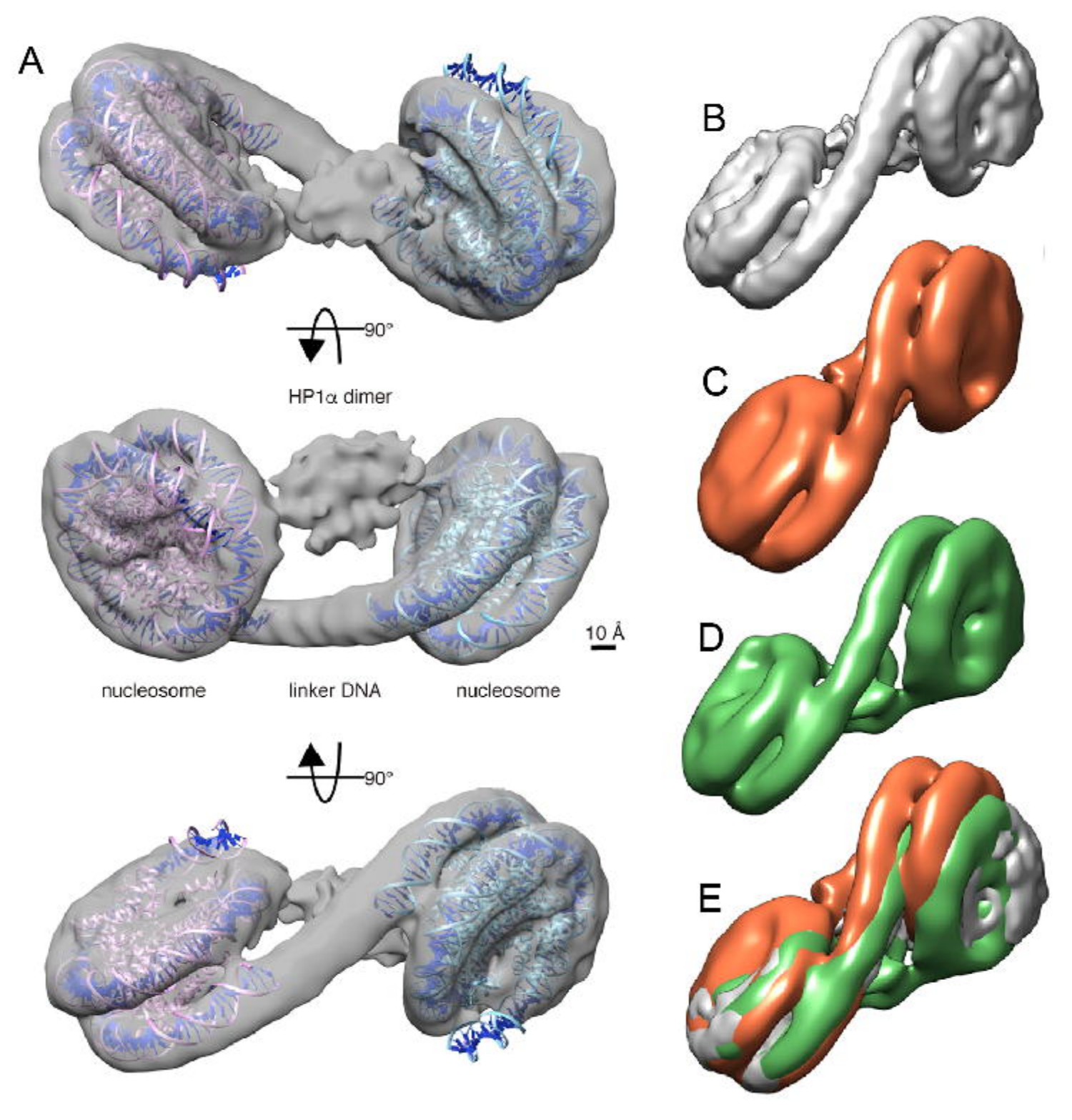
A
90°
HP1α dimer
10 Å
nucleosome
linker DNA
nucleosome
90°
B
C
D
E

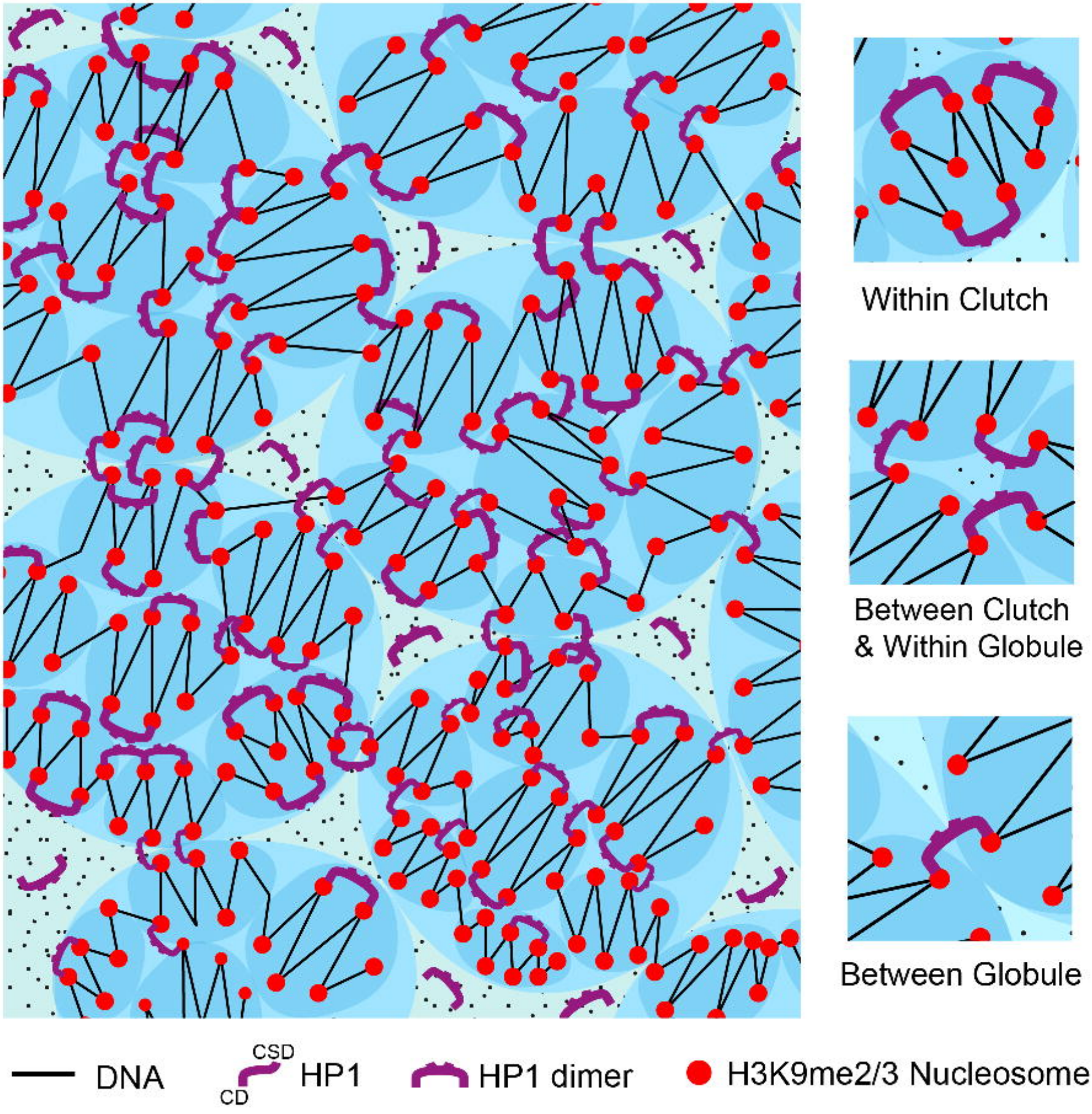
Within Clutch
Between Clutch
& Within Globule
Between Globule
DNA
CSD
CD
HP1
HP1 dimer
H3K9me2/3 Nucleosome

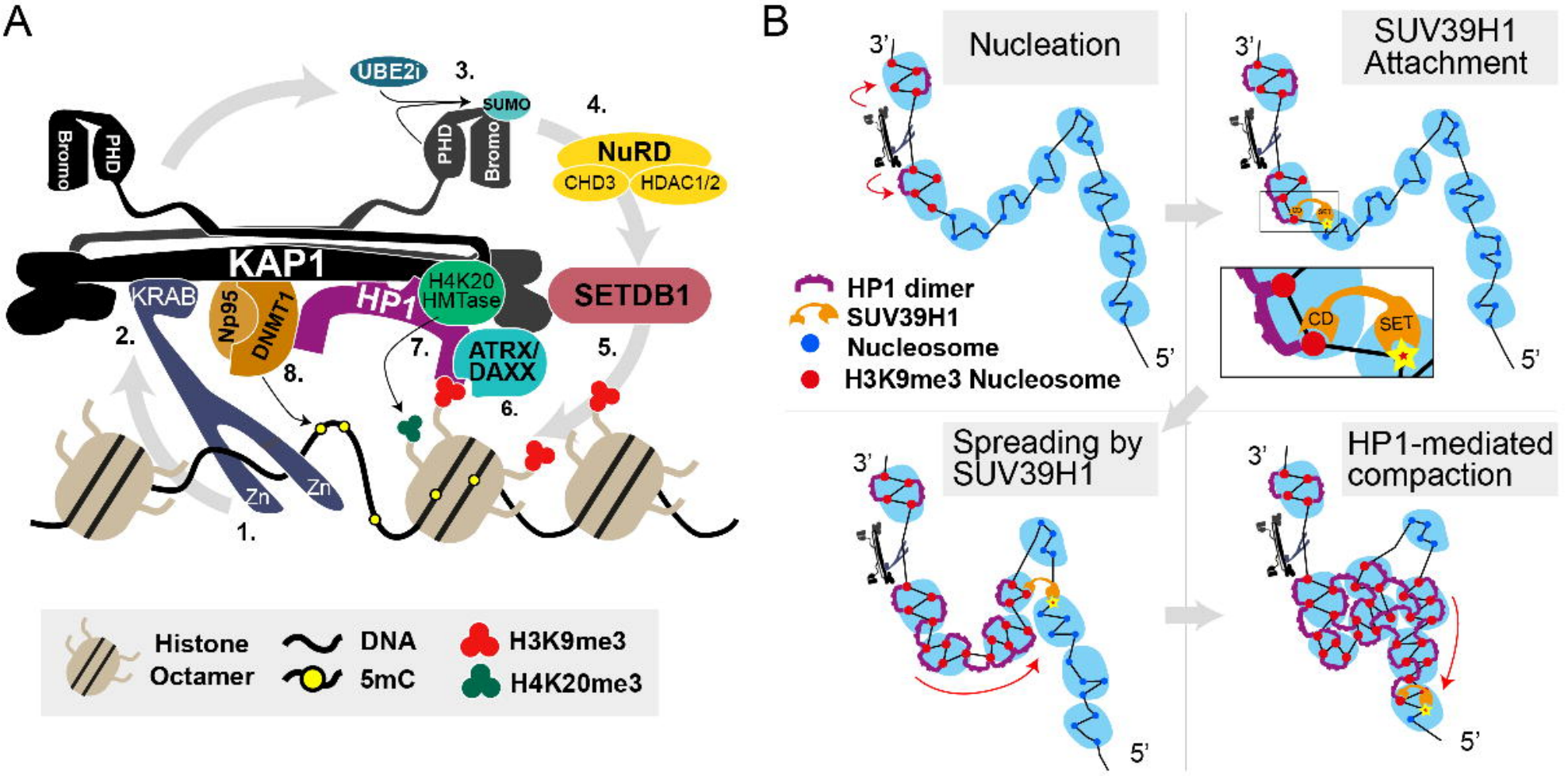
A
UBE2i
3.
SUMO
4.
Bromo
PHD
PHD
Bromo
NuRD
CHD3
HDAC1/2
KAP1
KRAB
Np95
DNMT1
HP1
H4K20
HMTase
SETDB1
2.
8.
7.
ATRX/
DAXX
5.
6.
Zn
Zn
1.
Histone
Octamer
DNA
5mC
H3K9me3
H4K20me3
B
Nucleation
SUV39H1
Attachment
3'
5'
CD
SET
HP1 dimer
SUV39H1
Nucleosome
H3K9me3 Nucleosome
Spreading by
SUV39H1
HP1-mediated
compaction

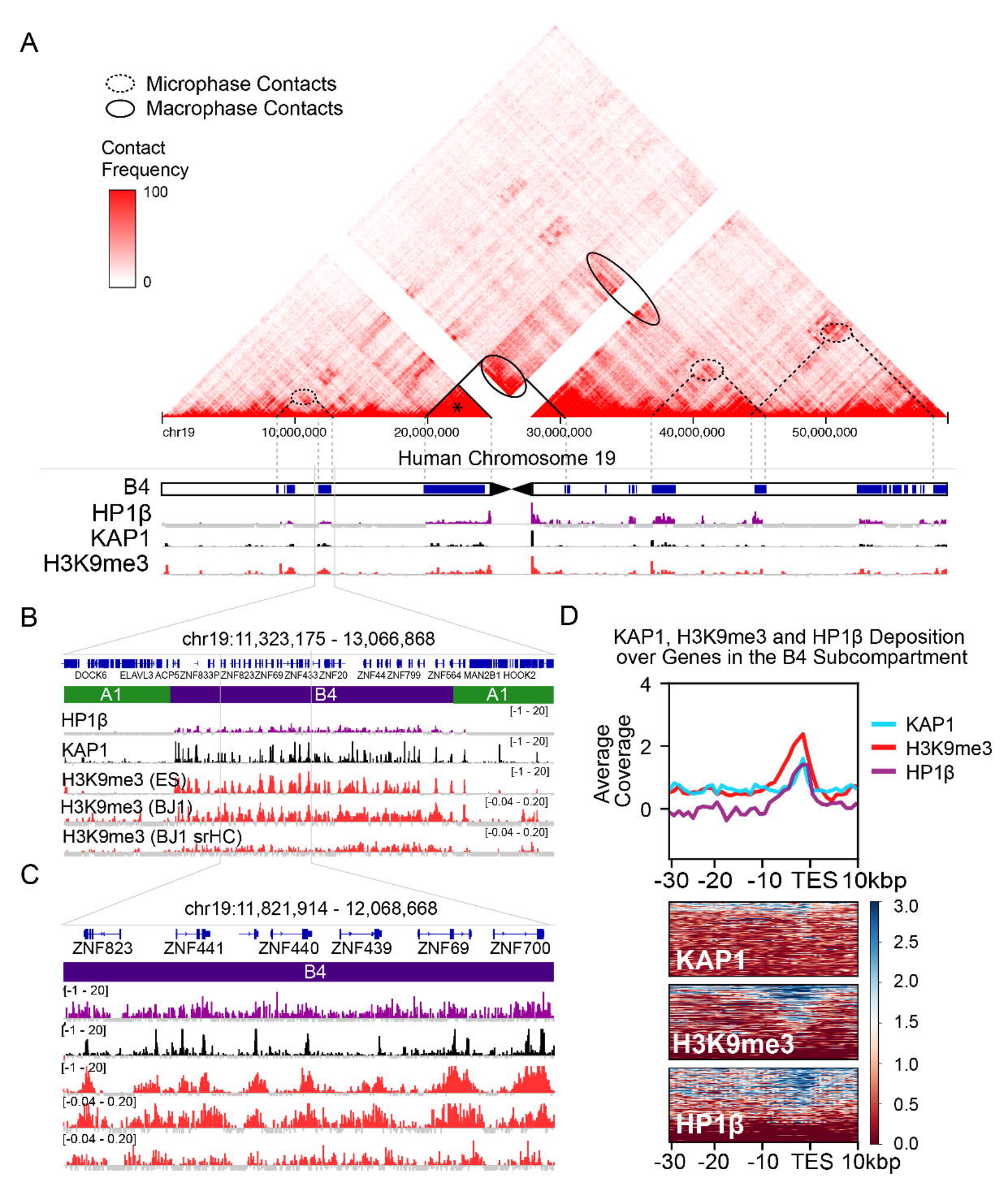
A
Microphase Contacts
Macrophase Contacts
Contact Frequency
100
0
chr19
10,000,000
20,000,000
30,000,000
40,000,000
50,000,000
Human Chromosome 19
B4
HP1β
KAP1
H3K9me3
B
chr19:11,323,175 - 13,066,868
DOCK6 ELAVL3 ACP5 ZNF833P ZNF823 ZNF69 ZNF433 ZNF20 ZNF44 ZNF799 ZNF564 MAN2B1 HOOK2
A1
B4
A1
HP1β
[-1 - 20]
KAP1
[-1 - 20]
H3K9me3 (ES)
[-1 - 20]
H3K9me3 (BJ1)
[-0.04 - 0.20]
H3K9me3 (BJ1 srHC)
[-0.04 - 0.20]
C
chr19:11,821,914 - 12,068,668
ZNF823 ZNF441 ZNF440 ZNF439 ZNF69 ZNF700
B4
[-1 - 20]
[-1 - 20]
[-1 - 20]
[-0.04 - 0.20]
[-0.04 - 0.20]
D
KAP1, H3K9me3 and HP1β Deposition over Genes in the B4 Subcompartment
Average Coverage
4
2
0
KAP1
H3K9me3
HP1β
-30 -20 -10 TES 10kbp
KAP1
H3K9me3
HP1β
3.0
2.5
2.0
1.5
1.0
0.5
0.0
-30 -20 -10 TES 10kbp

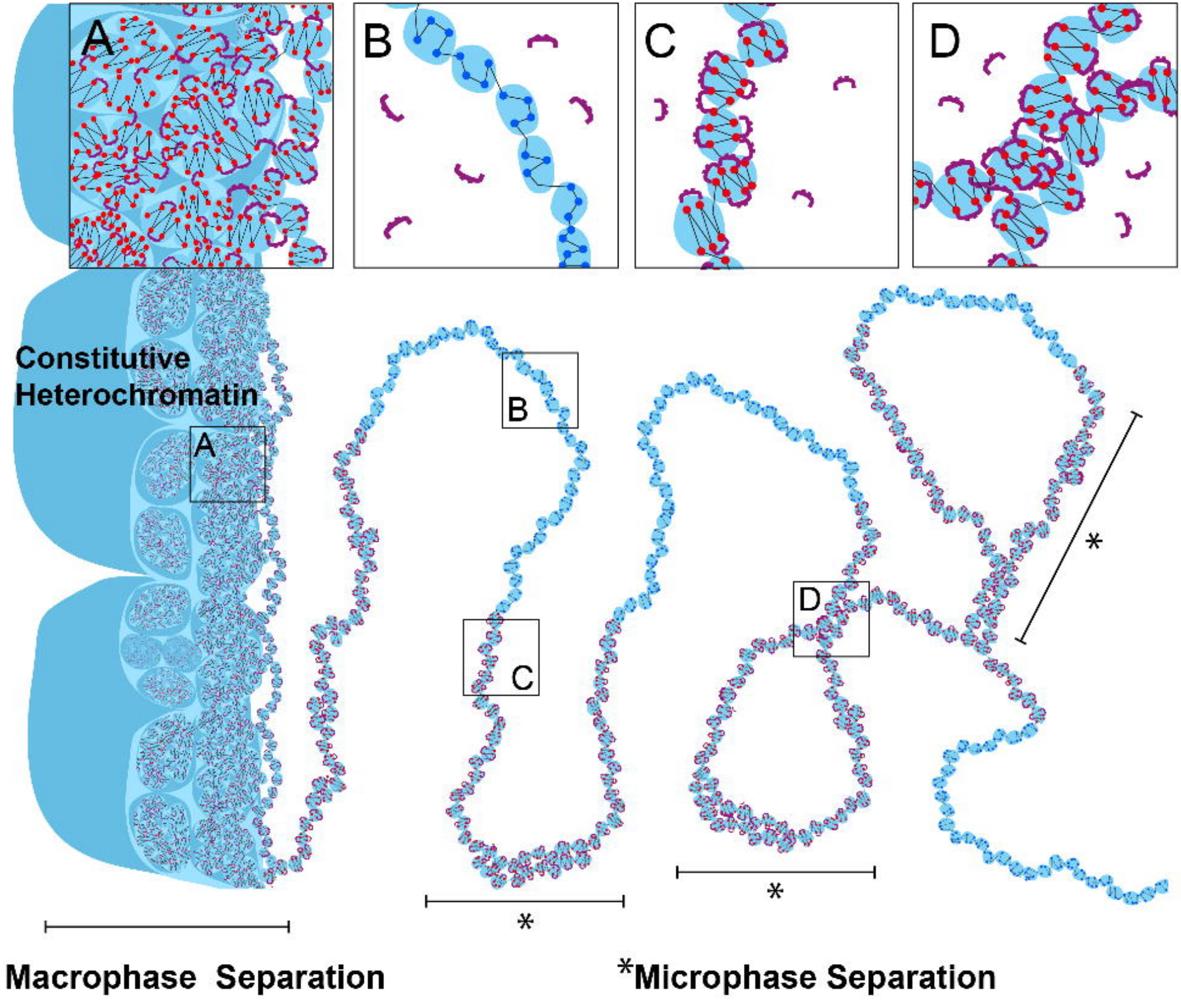
A
B
C
D
Constitutive Heterochromatin
A
B
C
D
*
*
*
Macrophase Separation
*Microphase Separation
DNA
CSD
CD
HP1
HP1 dimer
"Euchromatic" Nucleosome
H3K9me2/3 marked Nucleosome

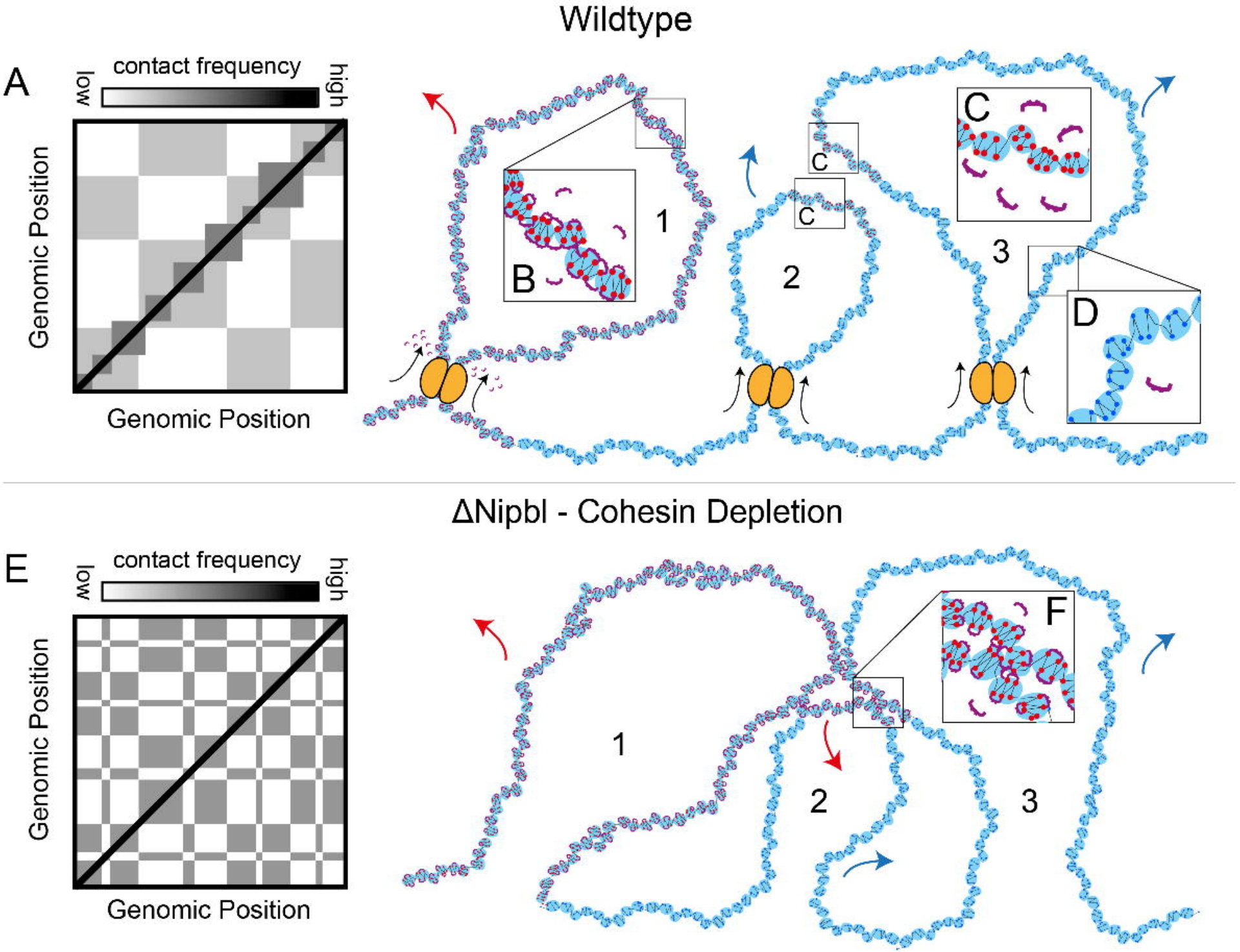
Wildtype
A
contact frequency
low
high
Genomic Position
Genomic Position
B
C
C
C
D
1
2
3
ΔNipbl - Cohesin Depletion
E
contact frequency
low
high
Genomic Position
Genomic Position
F
1
2
3